Published online 5 February 2020 *Nucleic Acids Research, 2020, Vol. 48, No. 6* **3053–3070**
doi: 10.1093/nar/gkaa054

Exo1 phosphorylation inhibits exonuclease activity and prevents fork collapse in *rad53* mutants independently of the 14-3-3 proteins

Esther C. Morafraile[1,†], Alberto Bugallo[1,†], Raquel Carreira[2], María Fernández[1], Cristina Martín-Castellanos[1], Miguel G. Blanco[2] and Mónica Segurado[1,3,*]

[1]Instituto de Biología Funcional y Genómica (CSIC/USAL), Campus Miguel de Unamuno, Salamanca 37007, Spain, [2]Departamento de Bioquímica y Biología Molecular, Centro de Investigación en Medicina Molecular y Enfermedades Crónicas (CIMUS) - Instituto de Investigación Sanitaria (IDIS), Universidad de Santiago de Compostela, 15782 Santiago de Compostela, Spain and [3]Departamento de Microbiología y Genética, Campus Miguel de Unamuno, Universidad de Salamanca, Salamanca 37007, Spain

Received December 23, 2019; Revised January 15, 2020; Editorial Decision January 16, 2020; Accepted January 20, 2020

ABSTRACT

The S phase checkpoint is crucial to maintain genome stability under conditions that threaten DNA replication. One of its critical functions is to prevent Exo1-dependent fork degradation, and Exo1 is phosphorylated in response to different genotoxic agents. Exo1 seemed to be regulated by several post-translational modifications in the presence of replicative stress, but the specific contribution of checkpoint-dependent phosphorylation to Exo1 control and fork stability is not clear. We show here that Exo1 phosphorylation is Dun1-independent and Rad53-dependent in response to DNA damage or dNTP depletion, and in both situations Exo1 is similarly phosphorylated at multiple sites. To investigate the correlation between Exo1 phosphorylation and fork stability, we have generated *phospho-mimic exo1* alleles that rescue fork collapse in *rad53* mutants as efficiently as *exo1-nuclease dead* mutants or the absence of Exo1, arguing that Rad53-dependent phosphorylation is the mayor requirement to preserve fork stability. We have also shown that this rescue is Bmh1–2 independent, arguing that the 14-3-3 proteins are dispensable for fork stabilization, at least when Exo1 is downregulated. Importantly, our results indicated that phosphorylation specifically inhibits the 5' to 3'exo-nuclease activity, suggesting that this activity of Exo1 and not the flap-endonuclease, is the enzymatic activity responsible of the collapse of stalled replication forks in checkpoint mutants.

INTRODUCTION

Conditions that perturb DNA replication are an important threat to genomic stability. The ability to overcome them depends on the S phase checkpoint, which is a surveillance mechanism that responds to replication perturbations and coordinates a global response to ensure successful chromosome replication and to preserve genome integrity and cell survival (1,2).

Commonly, cancer cells present a defective checkpoint pathway (3), which render these cells sensitive to chemotherapeutic agents that inhibit DNA replication. Therefore, it is important to understand the cellular mechanisms that sense and respond to replication perturbations to improve the efficiency of anti-cancer therapies. In addition, replication fork blockage is linked to the appearance of chromosomal rearrangements and breakage, which are an important source of genome instability (4) and it is well established that checkpoint pathways contribute to maintain genomic stability (5–7) and represent a barrier to carcinogenesis too (8,9).

The S phase checkpoint involves Mec1 and Rad53 kinases in *Saccharomyces cerevisiae* (2), corresponding to ATR and CHK1 in human cells (10–12), and to Rad3 and Cds1 in *Schizosaccharomyces pombe* (13,14). In conditions that threaten DNA replication, such as DNA damage or nucleotide depletion, the S phase checkpoint gets activated with the kinase Mec1 being recruited to stalled replication forks and the subsequent phosphorylation of the effector kinase Rad53 and the downstream kinase Dun1 (15,16). The checkpoint response regulates different processes such as in-

*To whom correspondence should be addressed. Tel: +34 923 294919; Fax: +34 923 224876; Email: monicas@usal.es
†The authors wish it to be known that, in their opinion, the first two authors should be regarded as joint First Authors.
Present address: Esther C. Morafraile, Wellcome Trust/Cancer Research UK Gurdon Institute, University of Cambridge, Cambridge CB2 1QN, UK.

© The Author(s) 2020. Published by Oxford University Press on behalf of Nucleic Acids Research.
This is an Open Access article distributed under the terms of the Creative Commons Attribution Non-Commercial License (http://creativecommons.org/licenses/by-nc/4.0/), which permits non-commercial re-use, distribution, and reproduction in any medium, provided the original work is properly cited. For commercial re-use, please contact journals.permissions@oup.com

hibition of mitosis, transcription of ribonucleotide reductase (RNR) and other genes involved in the DNA damage response (DDR) and inhibition of late origin firing (17–21). All of these processes contribute to cell survival, but it seems that preserving replication fork stability is critical (22). The S phase checkpoint preserves the integrity and functionality of DNA replication forks to ensure full chromosome replication after replication perturbations have been solved (23,24). In the absence of a functional checkpoint, replication forks are irreversibly damaged, a state known as fork collapse.

The nature of fork collapse in checkpoint mutants treated with the RNR inhibitor hydroxyurea (HU) is not well understood, but it is characterized by the presence of abnormal DNA structures, which have not been observed in wild-type cells. In particular, the collapse of stalled replication forks leads to a reduced percentage of DNA replication bubbles analysed by two-dimensional (2D) gel electrophoresis, together with an accumulation of unusual DNA replication intermediates at forks. These aberrant structures observed by electron-microscopy (EM) include a high proportion of stalled replication bubbles with long stretches of single-stranded DNA (ssDNA), and a smaller amount of forks with gaps and reversed forks (24–26).

The origin of these unusual structures is not clear, although different factors could contribute to their formation. One possibility is that, in the absence of a functional checkpoint, inappropriate exposure of replication intermediates at stalled forks may lead to degradation of the strands and the accumulation of ssDNA regions. This would be caused by replisome disassembling in checkpoint mutants (27–29), although it has been recently shown that the replisome remains stably associated with stalled forks in yeast and human cells (30,31); other possible scenario is the improper unwinding of the newly synthesized strands (32), or other unrevealed events. In any case, these abnormal DNA transitions would expose newly synthesized DNA to nucleolytic processing, leading to irreversible fork collapse (23,24).

One nuclease implicated in fork degradation is Exo1, a Rad2 family nuclease with a double strand-specific 5′ to 3′exonuclease and 5′flap endonuclease activities involved in different cellular processes and repair pathways, like Okazaki fragment maturation, telomere processing, mismatch repair, double-strand break (DSB) repair, and mitotic and meiotic recombination (33–40).

Fork collapse of *rad53* mutants exposed to HU or DNA damaging agents is dependent on the presence of Exo1, and thus, *EXO1* deletion preserves the stability of replication forks in *rad53* mutants in the presence of both HU and methyl methanesulphonate (MMS) (29,41). However, the requirements to maintain functional replication forks and survive to replication blockage seem to be different after exposure to MMS or HU. Thus, elimination of *EXO1* suppresses the defect in fork progression of *rad53* mutant cells in the presence of the DNA alkylating agent MMS and notably increases viability (41,42), while additional Exo1-independent mechanisms are required to permit replication-fork restart and viability after HU treatment (41). This additional mechanism depends, at least in part, on the Rad53-dependent induction of *RNR2*, *RNR3* and *RNR4* genes (17), as *RNR2–3-4* expression in the absence of Exo1 promotes replication resumption after fork stalling in *rad53* mutants and improves resistance to HU (43). New synthesis and activation of the RNR enzymatic complex might be especially important after a prolonged treatment with the inhibitor HU.

It has been proposed that Exo1 resects stalled and reversed forks in *rad53* cells treated with HU (44), and also that the nuclease activity of Exo1, together with Dna2 and Sae2, would counteract the generation of some of these abnormal replication intermediates, like the reversed forks (45). Thus, it is currently unclear whether these DNA structures are substrates or products of Exo1 activity, and the biochemical Exo1 activity responsible of fork degradation has not been determined yet.

In budding yeast, Exo1 is phosphorylated *in vivo* after DNA damage or telomeric stress by checkpoint kinases (46–49), and in human cells after fork stalling, EXO1 is also phosphorylated by the checkpoint machinery. In this case, ATR-dependent phosphorylation of Exo1 leads to ubiquitin-mediated degradation of the protein (50,51), whereas in yeast this regulatory mechanism has not been observed. In addition, human EXO1 undergoes CDK-dependent phosphorylation in S- and G2-phase, which modulates its recruitment to DNA during DSB resection (52). Mec1-dependent phosphorylation of yeast Exo1 was proposed to limit Exo1 activity at uncapped telomeres (47); but the biological consequences of this phosphorylation and, in particular, how could influence fork stability have not been clarified. In addition to phosphorylation, it has been recently reported that both yeast and human EXO1 are also SUMOylated in response to DNA replication stress (53), and proposed that sumoylation regulates human EXO1 stability and ubiquitin-mediated EXO1 degradation.

Also, it has been shown that Exo1 *in vivo* interacts with 14-3-3 proteins, both in yeast and mammalian cells (48). In yeast, this interaction is HU-dependent and it has been suggested that it modulates the phosphorylation of Exo1, which would limit its activity and, therefore, would influence fork stability and progression in response to DNA replication stress (48).

Despite all this information about EXO1 control in different conditions and systems, how checkpoint-dependent Exo1 regulation protects replication forks is not understood.

Here we have shown that Exo1 phosphorylation occurs with a similar pattern in response to MMS or HU treatment, and in both situations specifically depends on the checkpoint kinase Rad53. We have generated *exo1-phosphomimic* alleles that rescue fork collapse in *rad53* mutants in HU independently of the 14-3-3 proteins, arguing that Rad53-dependent phosphorylation of Exo1 is sufficient to restrain its deleterious action at stalled replication forks. Importantly, our results indicated that the phosphomimic Exo1–23D variant is deficient specifically in 5′-3′exonuclease activity, arguing that phosphorylation has a direct inhibitory effect on this catalytic activity of Exo1. In fact, both *in vivo* and *in vitro* data suggest that Exo1 flap-activity is not primarily involved in fork degradation and, points at the 5′-3′exonuclease activity as responsible of the collapse of stalled replication forks in checkpoint mutants.

MATERIALS AND METHODS

Strains and grow conditions

All yeast strains used in this work derive from W303 and are described in the Supplementary Table S1. Phospho-mutants *exo1–23D* and *exo1–23A* were constructed by delitto perfetto (54) using artificially synthesized genes made by GeneWiz carrying the modifications detailed in the Supplementary Table S2. The *exo1-D173A* and *exo1-E150D* alleles from YIp-exo1-D173A and YIp-exo1-E150D respectively (55) were used to replace the wild-type *EXO1* fragment by delitto perfetto (54). All the exo1-mutant strains were sequenced to verify correct replacement with the mutated fragments. The rest of the strains were constructed using standard techniques.

Cells were grown in YPD medium at 30°C and synchronized in G1 phase using the mating pheromone α-factor at 10 μg/ml. Then cells were released into S phase in medium with either 0.033% MMS or 0.2M HU.

For synthetic lethality analysis, a *rad27Δ* mutant strain was crossed with different *exo1* mutants of the opposite mating type to generate diploids that were tetrad dissected after sporulation to analyse the viability of the progeny.

Drop assay

Cell cultures were grown overnight until they reach the stationary phase and then 1:5 serial dilutions were spotted into YPD or YPD with HU or different concentrations of MMS, depending on the experiment. Lastly, plates were incubated at 30°C for 3 days.

Flow cytometry

10^8 cells were fixed in 70% ethanol after sample collection and then washed in 50 mM sodium citrate prior flow cytometry analysis. After the wash, cells were first treated with RNase A (0.1 mg/ml) and then with Proteinase K (0.8 mg/ml). Finally, cells were washed in 50 mM sodium citrate again and resuspended in 50 mM sodium citrate with 4 μg/ml of propidium iodide. Treated cells were then analysed in a Facscalibur flow cytometer (BD biosciences).

Protein electrophoresis, immunoblotting and immunoprecipitation

Protein extracts and electrophoretic conditions were performed as described (43). When specified, Phos-tag™ reagent (Wako chemicals, AAL-107) and $MnCl_2$ were added to 7.5% sodium dodecyl sulphate-polyacrylamide gelelectrophoresis (SDS-PAGE) gels to a final concentration of 5 mM and 160 nM, respectively. Proteins were separated at constant amperage of 30 mA per gel in a Miniprotean III (Bio-Rad) or at 60 mA per gel in a TV200 (SciePlas), both for 90 min. After the electrophoresis, the gel was incubated in standard transfer buffer with ethylenediaminetetraacetic acid (EDTA) at 0.1M for 30 min, followed by three washes with transfer buffer for 10 min. Then, the gel was transferred to a PVDF membrane (Immobilon-P, Millipore) in a Mini-Transfer system (Bio-Rad) at 200 mA overnight. Exo1-MYC was detected using the mouse monoclonal α-MYC antibody clone 4A6 (Millipore; dilution 1:1000). Detection of Rad53 was performed using a rabbit polyclonal antibody provided by J. Diffley (JDI48; dilution 1:1000) and PGK was detected using the mouse polyclonal antibody 22C5 (Sigma; dilution 1:20 000). The corresponding protein A or α-mouse secondary antibody coupled with horseradish peroxidase were used at 1:5000 dilution, and finally immunoreactive bands were visualized by enhanced chemiluminescence (ECL, GE Healthcare). Alternatively, goat α-mouse secondary antibodies coupled to Alexa Fluor Plus 800 (Thermo, dilution 1:5000) were employed for protein detection on an Odyssey scanner (Li-Cor Biosciences).

Immunoprecipitations were performed as described (56). PhosSTOP phosphatase inhibitors (Roche) were added in lysis and washing buffers as indicated by the manufacterer. Exo1-MYC was pulled down with 10 μg of α-MYC antibody (Millipore, clone 4A6) and 15 μl of Protein G loaded Dynabeads (Invitrogen), and Bmh1-PK was detected by immunoblot with the mouse α-V5-TAG antibody (AbD Serotec dilution 1:20 000).

Nuclease activity assays

Protein extracts were made as for co-immunoprecipitations (56) but the lysis buffer was supplemented with 200 mM potassium acetate. To measure nuclease activity, MYC-tagged Exo1 variants were immunoaffinity purified with α-MYC antibody (9E10, Cancer Research UK) coupled to agarose beads with the AminoLink kit (Thermo Scientific, 44894). A total of 20 μl 50% bead slurry and 500 μl cell extracts were mixed for 30 min at 4°C and washed twice with lysis buffer containing 200 mM potassium acetate and twice with lysis buffer containing 500 mM potassium acetate. The beads were then equilibrated in 1 ml reaction buffer (25 mM Tris–HCl pH 8.0, 75 mM NaCl, 1 mM DTT, 10 mM MgCl2, 4% glycerol) and split for western blot analysis (20%) and nuclease assays (80%). Synthetic DNA substrates were prepared as described (57), employing the following oligonucleotides: (i) splayed arm, 5′FAM-A6 (5′-6FAM-A*T*T*GGTTA TTTACCGAGCTCGAATTCACTGG-3′, with asterisks indicating phosphorothioate linkages) + A9 (5′-CCAGTGAATTCGAGCTCGGTACCCGC TAGCGGGGATC CTCTA-3′); (ii) 5′-recessed dsDNA, A6–3′FAM (5′-ATTGGTTATTTACCGAGCT CGAATTCACTGG-6FAM-3′) + A6-comp-poliT (5′-CCAGTGAATTCGAGCT CGGTAAATAACCAA TTTTTT-3′); (iii) dsDNA, X01 (5′-ACGCTGCCGAA TTCTACCAGTGCCTTGCTAGGACATCTTTGCCCA CCTGCAGGTTCACCC-3′) + X01-comp (5′- GGGT GAACCTGCAGGTGGGCAAAGATGTCCTAGCAA GGCACTGGTAGAATTCGGCAGCGT-3′); (iv) ssDNA, X0–1. Beads for nuclease assays were resuspended in 5 μl 2× reaction buffer and 5 μl DNA mix (20 nM fluorescently labelled substrate, with 10 nM competitor ssDNA and 10 nM competitor dsDNA) and incubated for 10 min at 30°C with gentle agitation. For analysis of exonuclease activity, reactions were stopped with 1.3 μl STOP solution (0.5 mg/ml proteinase K, 0.5% SDS) and incubated for 20 min at 37°C. After addition of 2 μl native loading buffer (15% Ficoll-400 in 60 mM EDTA, 20 mM Tris–HCl pH

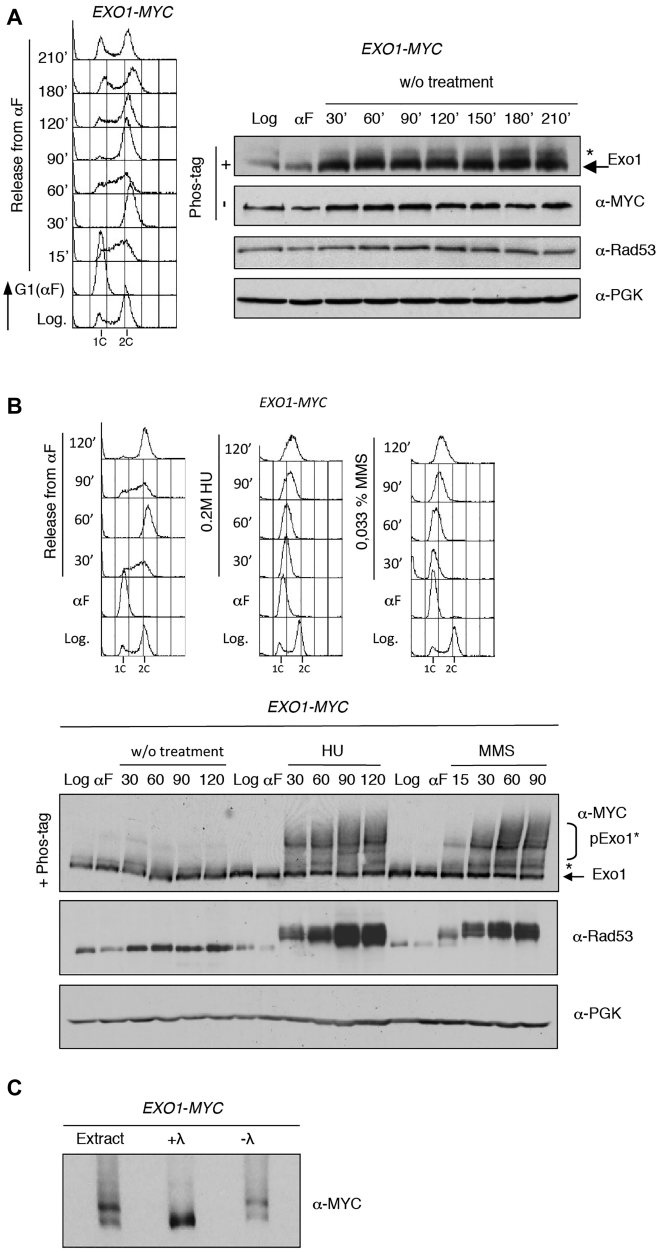

Figure 1. Similar Exo1 phosphorylation pattern in response to dNTPs depletion or DNA damage. (**A**) An *EXO1-MYC* culture was synchronized in G1 with α-factor pheromone and released into YPD medium for 210 min. Samples were taken at the indicated times for flow cytometry analysis (left panel) and immunoblot analysis (right panel). Exo1-MYC was detected with α-MYC antibody, and Rad53 and PGK were detected with α-Rad53 and α-PGK antibodies respectively. Exo1-MYC was analysed during unperturbed conditions in acrylamide gels in the absence or presence of Phos-tag (indicated as − or +), and in the last case, Exo1 showed a constitutive single band (arrow) plus a weaker upper band (asterisk). (**B**) *EXO1-MYC* cells were blocked in G1 with α-factor and then released into YPD medium or in YPD containing either 0.2M HU or 0.033% MMS. The percentage of budded cells after 120 min from α-factor release in non-treated, HU or MMS-treated cells was 98, 96 and 97%, respectively. Samples were taken at G1 and at the indicated times during S phase for DNA content analysis (upper panel) and immunoblot analysis for Exo1-MYC, Rad53 and PGK as indicated in (A) (lower panel). For Exo1-MYC analysis, protein samples were run in Phos-tag gels and, like in (A), the arrow and the asterisk points at the constitutively detected Exo1 bands, whilst the low mobility bands marked as pExo1 (crochet) are specifically detected in the presence of HU or MMS. (**C**) λ-phosphatase assay of Exo1. Protein extracts from HU-treated cells were either untreated, treated with λ-phosphatase (+) or just with the phosphatase's buffer (−). After the treatment, the extracts were run in a Phos-tag gel and Exo1-MYC was detected by immunoblot with α-MYC antibody.

8.0, 0.48% SDS) reaction products were separated by 10% native PAGE in 1× TBE (90 mM boric acid, 90 mM Tris base, 2 mM EDTA). For analysis of endonuclease activity, reactions were stopped by the addition of 1 volume of 2× formamide-loading buffer (80% formamide in 1× TBE), boiled at 99°C for 5 min and products were separated in 16% polyacrylamide, 7M urea-denaturing gels in 1× TBE. Fluorescent products were detected by scanning fresh gels at 488 nm in a Typhoon FLA9500 (GE Healthcare).

λ-phosphatase assay

Protein extracts were prepared as described (43) in the following buffer (6.6% Glycerol, 62.5 mM Tris base, 3% SDS) and, then, diluted in RIPA buffer (50 mM Tris-HCL pH 8, 150 mM NaCl, 1% Np-40, 0.5% sodium deoxycholate, 0.1% SDS). The resulting extracts were either treated with the λ protein phosphatase kit (New England Biolabs) or only with the included buffer. Samples were then run in a Phos-tag gel.

Two-dimensional electrophoresis

Genomic DNA was isolated using the QIAGEN Blood & Cell Culture DNA Midi Kit following the manufacturer's instructions. Then, the purified DNA was digested using XbaI and EcoRI, and separated by neutral/neutral 2D agarose gel electrophoresis as previously described (58). The DNA was transferred to a nylon membrane (Amersham Hybond XL) for Southern Blotting. The fragments of interest were detected with a P^{32} labelled DNA probe. Replication intermediates were quantified by calculating the percentage radioactivity signals in specific recombination intermediates relatively to the monomer spot as described (59).

RESULTS

Exo1 is phosphorylated with similar dynamics during S phase in response to DNA damage or nucleotide depletion

We started analysing post-translational modifications of Exo1 during the cell cycle, in normal or perturbed conditions in budding yeast. In the first place, we analysed Exo1 expression and presence of modifications during the cell cycle in unperturbed conditions. An asynchronous culture of an Exo1-MYC strain was synchronized in G1 with α-factor mating pheromone and released into fresh medium for 210 min, which covers approximately two cell cycles based on flow cytometry and percentage of budded cell analysis (Figure 1A, left panel and Supplementary Figure S1A). Protein samples were taken at different time points to examine Exo1 regulation by SDS-PAGE (Figure 1A, right panel), and this analysis showed first, that Exo1 was present at similar levels through the cell cycle as a single prominent

band and a weaker upper band (arrow and asterisk, respectively, in Figure 1A) and second, that Exo1 mobility did not change significantly at any stage in the absence or presence of Phos-tag. As expected in the absence of genotoxic stress, immunoblot analysis of Rad53 showed absence of Rad53 phosphorylation during the experiment.

Next, we compared Exo1 electrophoretic migration during S phase in normal conditions and in response to nucleotide depletion or DNA damage. In this case, G1 blocked cells were released into S phase in fresh medium or in the presence of 0.2M HU or 0.033% MMS, and samples were taken to monitor DNA content and Exo1 modifications along the experiment (Figure 1B). In these three situations, the cells entered normally into S phase, as indicated by the estimation of the budding index in all cases (>95% budded cells after 120 min from α-factor release). Regarding Exo1 post-translational modifications, as cells entered S phase in the presence of either HU or MMS, a new set of bands was detected but only when protein samples were analysed in SDS-PAGE in the presence of Phos-tag (Figure 1B and Supplementary Figure 1B-C), indicating that the protein is modified at several sites in both conditions. A very similar pattern of modified bands was observed in the samples treated with HU or MMS, and in both situations the Exo1 shift was detected from the beginning of S phase and it remained as long as HU or MMS were present in the culture medium. The Exo1 shift correlated with checkpoint activation under these conditions, as observed by analysing Rad53 phosphorylation by immunoblot (Figure 1B). In HU and MMS-treated samples, we observed Exo1 protein that remained unmodified, and so it was present at the same position than Exo1 protein in the untreated samples (arrow and asterisk in Figure 1B). Phosphatase treatment of protein extracts from HU-treated *EXO1-MYC* yeast cells converted the slower migrating bands into a single faster band (Figure 1C), indicating that the observed protein modifications correspond to Exo1 phosphorylation. Therefore, our results indicate that Exo1 phosphorylation takes place with similar kinetics during S phase in response to nucleotide depletion and DNA damage.

Role of Mec1, Rad53 and Dun1 kinases in Exo1 phosphorylation in response to DNA damage or replicative stress

Although previous studies have shown that after genotoxic stress Exo1 phosphorylation is dependent on checkpoint kinases (46–49), the contribution of Mec1, Rad53 and Dun1 kinases to Exo1 phosphorylation under DNA damage or nucleotide depletion has not been clarified. To answer this point, we have compared Exo1 phosphorylation in response to MMS or HU treatment in checkpoint proficient, *dun1Δ*, *rad53Δ* and *mec1Δ* cells (all the strains share a *sml1Δ* background to allow survival of *mec1Δ* and *rad53Δ* mutants). All the strains were synchronized in G1 by α-factor treatment and then released into S phase in the presence of MMS or HU. Flow cytometry analysis indicated that in the four strains DNA synthesis is blocked by HU, and DNA replication of damaged DNA proceeds very slowly in *sml1Δ* and *dun1Δ* mutants, and faster in *rad53Δ* and *mec1Δ* cells (Figure 2A and B), due to their inability to inhibit late origin firing as previously reported (23). Immunoblot analysis showed that whereas in the absence of Dun1 the Exo1 phosphorylation pattern is very similar to the one in the control strain (*sml1Δ* cells), the absence of Rad53 or Mec1 abolishes Exo1 phosphorylation in both situations, and that was obviously concomitant with lack of Rad53 phosphorylation (Figure 2A and B). Given that Rad53 is downstream Mec1 in the checkpoint-signalling pathway and Dun1 does not seem involved, our results indicate that Exo1 phosphorylation in response to DNA damage or nucleotide depletion is primarily Rad53-dependent.

Exo1 is phosphorylated at multiple sites in response to DNA damage or nucleotide depletion

If Exo1 suffers multiple phosphorylations after checkpoint activation and it is Rad53 dependent, it would be useful to identify all the relevant Rad53-dependent phosphorylation sites to be able to analyse the role of this phosphorylation in the regulation of the protein, and by extension in fork stability. Four major phosphorylation sites have been previously identified in Exo1 after MMS exposure or telomere uncapping, serines S372, S567, S587 and S692, (46,47); however, when these four residues were mutated to generate phospho-mimic mutants, the resulting *exo1–4SD* alleles showed a significantly milder phenotype than the one conferred by *EXO1* deletion (47,60), suggesting that although phosphorylation seems to inhibit protein function, phosphorylation at these four sites is not sufficient for a complete regulation of the protein and Exo1 might be phosphorylated at additional sites.

Thus, to identify additional Rad53-dependent phosphorylation sites, we performed an *in vitro* kinase assay with purified Rad53 and a cellulose membrane containing an array of peptides corresponding to the entire Exo1 amino acid sequence, and we identified 6 Ser/Thr that were phosphorylated by Rad53 *in vitro* (Supplementary Figure S2A). Two of these phosphorylation sites, S372 and S587, coincided with previously reported sites phosphorylated *in vivo* (46,47). When these six residues were converted to alanine, that blocks phosphorylation, the corresponding Exo1–6A protein showed a significant decrease in the phosphorylation shift upon MMS treatment (Supplementary Figure S2B). However, the substitution of these six Ser/Thr residues for aspartic acid, whose negative charge mimics phosphorylation of the residue, did not suppress replication fork collapse in *rad53* mutants (Supplementary Figure S2C), contrary to what *EXO1* deletion does, questioning if Exo1 phosphorylation by Rad53 was inhibiting the deleterious effect of Exo1 in fork integrity. One explanation for this phenotype might be that in the absence of the preferential phosphorylation sites, additional sites can be phosphorylated, or alternatively, additional phosphorylation sites may have been missed in our analysis. In fact, a residual phosphorylation shift can be observed in *exo1–6A* extracts upon MMS treatment (Supplementary Figure S2B).

To overcome this problem, and considering that three different approaches ((46,47) and this work) failed to detect all the possibly functional phosphorylation residues in Exo1, we decided to substitute for either alanine or aspartic acid the serines or threonines residues that follow the amino acids motif Ser/Thr-Ψ, in where the Ψ is an hydrophobic

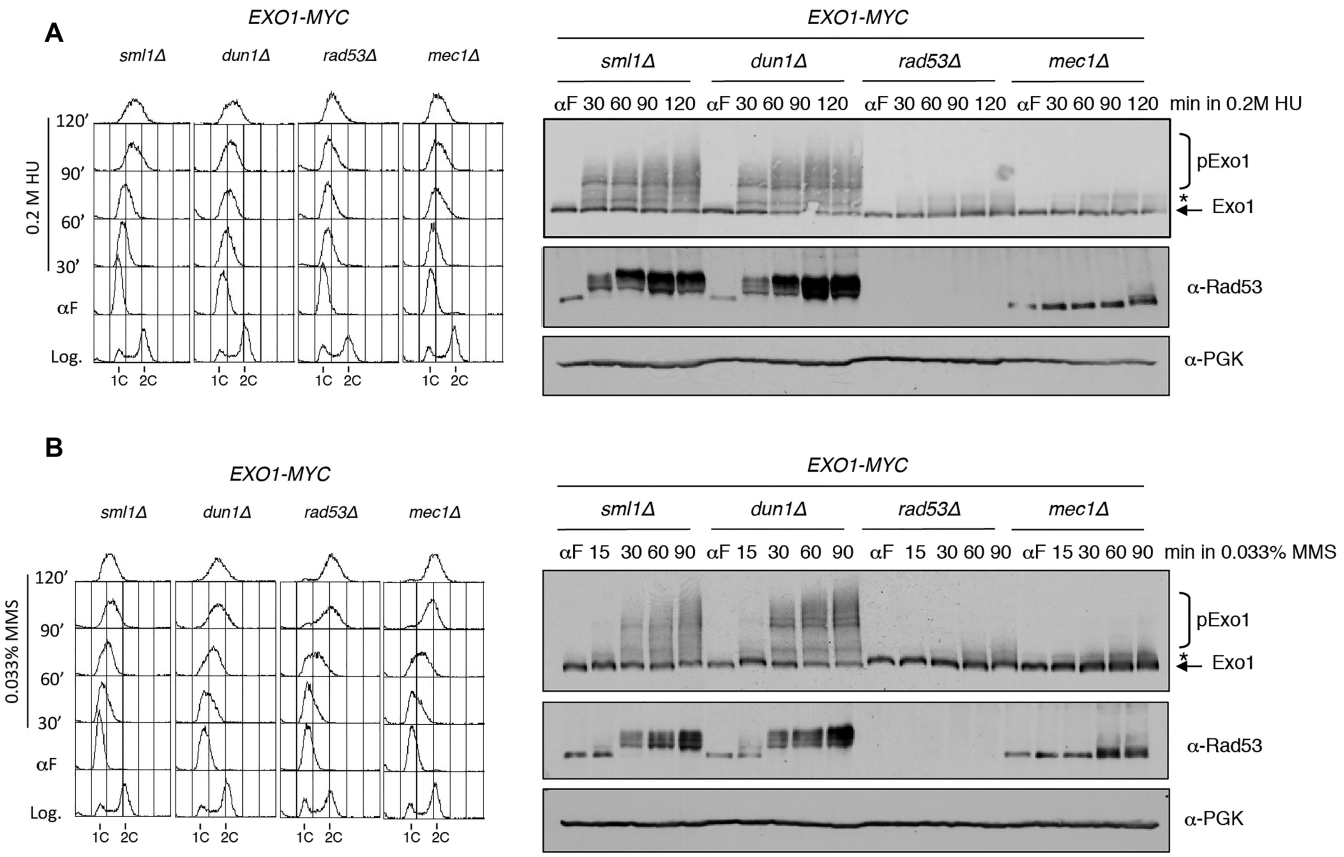

Figure 2. Exo1 phosphorylation is Rad53 dependent in response to dNTPs depletion or DNA damage. *sml1Δ*, *sml1Δ dun1Δ*, *sml1Δ rad53Δ* and *sml1Δ mec1Δ* strains were synchronized with α-factor and released into YPD medium in the presence of either 0.2M HU (**A**) or 0.033% MMS (**B**), and samples were taken at the indicated times. Flow cytometry analysis is shown in left panels, whilst immunoblots of protein extracts for Exo1-MYC, Rad53 and PGK are shown in right panels. For Exo1-MYC analysis, proteins were resolved on a Phos-tag polyacrylamide gel.

amino acid, described for potential Rad53 phosphorylation sites (46). Exo1 contains 702 amino acids residues, from which 97 are serines and threonines, and 23 of them fulfil this motif. Most of these 23 Ser/Thr residues were located in the C-terminal region, with only a few sites located in the N-terminal portion of the protein and none of them were altering the conserved nuclease consensus sequence (55). It has been shown that deletion of both *EXO1* and the flap-endonuclease *RAD27* is lethal, presumably because a defective processing of Okazaki fragments (36,61); however, yeast strains expressing *exo1–23A* or *exo1–23D* did not show synthetic lethality in combination with *RAD27* deletion (Figure 3A and Supplementary Figure S3A-B), indicating that the Exo1–23A and Exo1–23D proteins are capable to perform an essential function, likely Okazaki fragment maturation, and therefore, the 23 Ser/Thr residues selected for the analysis are not critical for protein function. When the phosphorylation status of these mutant alleles was examined, we observed that in the *exo1–23A* allele the phosphorylation shift of the protein was abolished in Phos-tag SDS-PAGE after both HU or MMS treatment (Figure 3B and C, respectively), indicating that most of the *in vivo* phosphorylation sites have been eliminated. As expected, the migration of the Exo1–23D protein was slower than Exo1 or Exo1–23A proteins at any time point, due to the negative charge conferred by the aspartic acid residues. Moreover, the electrophoretic mobility of Exo1–23A o Exo1–23D proteins was undistinguishable in the presence or absence of Rad53, indicating the lack of regulation by phosphorylation from this kinase in these mutants (Figure 3D).

An *exo1-23D* phospho-mimic allele suppresses fork collapse and improves survival in *rad53* mutants in HU

To examine the correlation between Exo1 phosphorylation and fork stability, we analysed the stability of replication forks by 2D gel in *rad53* mutants carrying these different phospho-mutant versions of Exo1.

To this end, *rad53Δ, rad53Δexo1Δ, rad53Δexo-23A and rad53Δexo-23D* cells were synchronized in G1 phase and released into rich medium containing 0.2 M HU for 2 h, and DNA content was measured by flow cytometry every 30 min (Supplementary Figure S4A). We analysed replication intermediates arising from the activation of the early origin ARS305, and we observed that in all cases replication bubbles accumulates within the fragment from 30 to 60 min after G1 release, due to replication fork stalling in the presence of HU. In *rad53Δ* cells replication bubbles are barely detectable from 90 min onwards and large Ys notably decrease, due to the collapse of the replication forks in the absence of a functional checkpoint (24), whereas in *rad53Δ exo1Δ* cells replication bubbles and large Ys remain

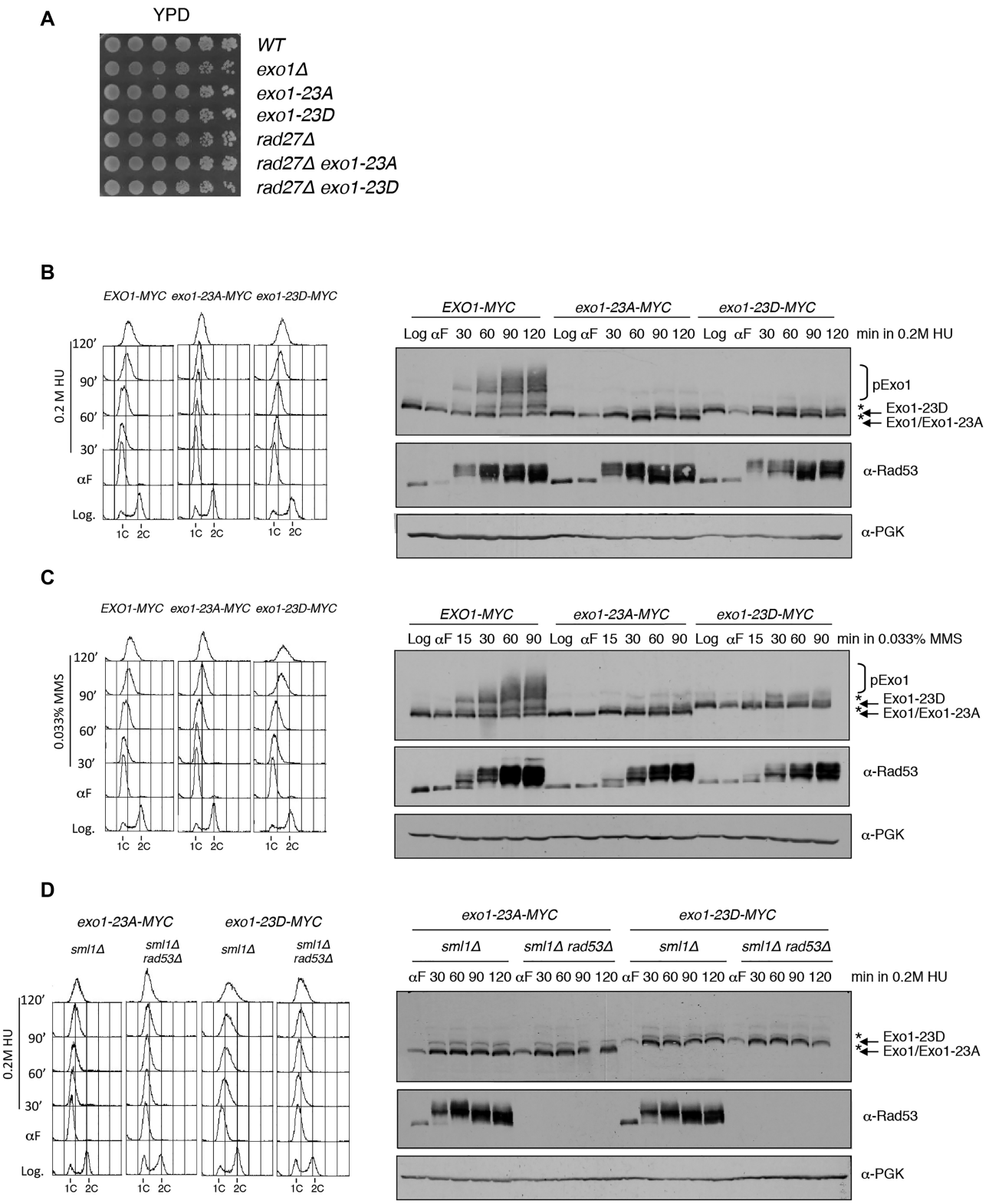

Figure 3. Analysis of viability and electrophoretic mobility of Exo1-phosphorylation mutants. (**A**) Drop assay of *exo1Δ, exo1–23A, exo1–23D*, *rad27Δ*, *rad27Δ exo1–23A* and *rad27Δ exo1–23D* strains. 1:5 serial dilutions of the indicated strains were spotted on YPD plates and incubated at 30°C for 3 days. (**B** and **C**) *EXO1-MYC*, *exo1–23A-MYC* and *exo1–23D-MYC* cells were synchronized with α-factor and released into YPD in the presence of either 0.2M HU (B) or 0.033% MMS (C), and samples were collected at the indicated times. Left panels show DNA content analysed by flow cytometry and right panels show immunoblots of Exo1-MYC, Rad53 and PGK. A Phos-tag gel was used for Exo1-MYC western blot analysis. (**D**) *sml1Δ exo1–23A-MYC, sml1Δ rad53Δexo1–23A-MYC, sml1Δ exo1–23D-MYC* and *sml1Δ rad53Δexo1–23D-MYC* cells were synchronized with α-factor and released in the presence of 0.2M HU. DNA content (left panel) and protein analysis (right panel) of the indicated samples were performed as in B and C.

stable through the experiment indicating that *EXO1* deletion suppresses fork collapse in HU as previously described (29). Interestingly, the *exo1–23D* phospho-mimic allele also suppresses fork collapse in *rad53Δ* mutants very efficiently, whereas the *exo1–23A* allele does not (Figure 4A and Supplementary Figure S4B). These results argue that Rad53 regulates fork stability after stalling mainly through Exo1 phosphorylation.

EXO1 deletion suppresses fork collapse but is completely ineffective in suppressing the sensitivity of *rad53* mutants to HU (41), and therefore, an Exo1-independent mechanism might be additionally required to support cell survival in the presence of HU. In fact, it has been shown that both Rad53-dependent negative regulation of Exo1 and RNR induction are important mechanisms for the viability of *rad53* mutants in the presence of replicative stress (43). This enzymatic complex is the target of HU (62), and on top of preserving stable replication forks in *rad53exo1* cells, new expression of RNR seems to be important to promote DNA synthesis, which is essential for cell viability after HU-induced stalling (43).

Similar to *EXO1* deletion, *exo1–23D* phospho-mimic allele also suppresses fork collapse (Figure 4A) but it does not rescue survival in *rad53* mutants in HU (Supplementary Figure S5). As we were interested in the role of Exo1 phosphorylation in fork stability and, perhaps, in cell survival in the presence of HU, we performed an HU-sensitivity assay with *rad53Δ, rad53Δ exo1Δ, rad53Δ exo1–23A* and *rad53Δ exo1–23D* strains in conditions that induce RNR or not. In these strains, the *RNR2*, *RNR3* and *RNR4* genes were expressed from the inducible *GAL1–10* promoter. Our results recapitulated that the combination of *EXO1* deletion and RNR expression significantly improved resistance to HU in a galactose-dependent manner, and the same was true with the *exo1–23D* allele but not with the *exo1–23A* allele (Figure 4B). These results indicated that Exo1 phosphorylation promotes fork stability and resistance to HU in *rad53Δ* mutants. However, as mentioned above, cell viability in the presence of HU requires also Exo1-independent mechanisms, such as RNR expression, between others.

exo1-23D phospho-mutant cells are impaired in the repair of MMS-induced DNA lesions but are proficient in Okazaki fragment maturation

To understand how replication fork stability was rescued in *rad53* mutants by *exo1–23D*, but not by the *exo1–23A* allele, we examined the properties of these Exo1 phospho-mutants. Regarding sensitivity to MMS, *exo1–23A* or *exo1–23D* mutant strains exhibited different phenotypes. Thus, the *exo1–23A* allele was not sensitive to MMS, whereas the phospho-mimic *exo1–23D* allele showed a significant sensitivity to MMS, similarly to the one observed in an *EXO1* deletion strain (Figure 5A). Exo1 activity is involved in the repair of MMS lesions, and therefore, is expected to be beneficial for viability in the presence of this drug (39). So, the MMS sensitivity of the *exo1–23D* allele suggests that phosphorylation might impair the activity of Exo1 involved in repair. To test this possibility, we compared the MMS sensitivity of this *exo1–23D* allele and some nuclease deficient mutants of Exo1 previously described, such as *exo1-D173A* and *exo1-E150D* (55). The biochemical characterization of these mutants have previously shown that the *exo1-D173A* allele was completely defective for both the dsDNA 5′-3′ exonuclease and flap-endonuclease activities, whereas the *exo1-E150D* was deficient for dsDNA 5′-3′ exonuclease activity but retained substantial flap-endonuclease activity (55). Thus, we compared the MMS sensitivity of wild-type *EXO1*, *exo1–23A, exo1–23D, exo1-D173A, exo1-E150D* and *exo1Δ* strains. We first discarded a negative effect of the MYC epitope in protein function (Supplementary Figure S6A), and we checked by western blot that the level of Exo1–23A and Exo1–23D proteins was like the Exo1-wild-type version, both in exponentially growing cells or in response to genotoxic treatment during S phase (Supplementary Figure S6B). Therefore, any observed differences in MMS sensitivity would not be attributed to different Exo1 protein levels in these phospho-mutants. As shown in Figure 5B, all the strains grew with similar rates on rich media (YPD), but *exo1-D173A* and *exo1-E150D* strains exhibited a marked sensitivity to MMS as reported previously (55), comparable with the one showed by the *exo1Δ* strain. Interestingly, independently of having flap-endonuclease activity or not, both nuclease mutants were similarly sensitive, supporting that the exonuclease activity is the one involved in MMS resistance. Therefore, if viability in MMS correlates with a proficient 5′-3′ exonuclease activity, the viability drop of the *exo1–23D* mutant, similar to the one observed in *exo1-D173A, exo1-E150D* and *exo1Δ* strains, argues that this strain might be also deficient in exonuclease activity. This is not the case for *exo1–23A* mutants that show no sensitivity to MMS.

DNA resection generates ssDNA, which is a signal to trigger DNA damage checkpoint activation (63), and it has been recently reported that Rad53 phosphorylation during S phase in the presence of MMS lesions is dependent on Exo1 activity (49). Therefore, we reasoned that a defective 5′-3′ exonuclease *exo1* allele, would affect checkpoint activation. To test this idea, we compared Rad53 phosphorylation in *EXO1*$^{+}$, *exo1Δ*, *exo1-E150D*, *exo1–23D* and *exo1–23A* strains during S phase in response to MMS treatment. Our results indicated that although checkpoint activation was not compromised in any of the strains, Rad53 phosphorylation was delayed at early time points in the *exo1-E150D* and *exo1–23D* strains, just like the *exo1Δ* strain, compared with an *EXO1*$^{+}$ or an *exo1–23A* strain, in which Rad53 phosphorylation was observed at 15 min after entry into S phase in the presence of MMS (Figure 5C, asterisks). In *exo1-E150D* and *exo1–23D* strains, Rad53 phosphorylation was not clearly detected until 30 min and beyond, similarly as shown in the absence of Exo1 (Figure 5C).

In G1, ssDNA arising from DNA lesions also triggers checkpoint activation in an Exo1-dependent manner (64), and, in particular, MMS lesions induced during G1 led to checkpoint activation during the next replication cycle (49). In this case, a marked delay in checkpoint activation was shown in the absence of Exo1 (49), and therefore, we decided to corroborate our previous result (Figure 5C) by analysing Rad53 phosphorylation in the same Exo1 mutants under these conditions. In this case, we observed that Rad53 phosphorylation was rapidly reached at 15 min after release from G1 in an *EXO1*$^{+}$ or an *exo1–23A* strain,

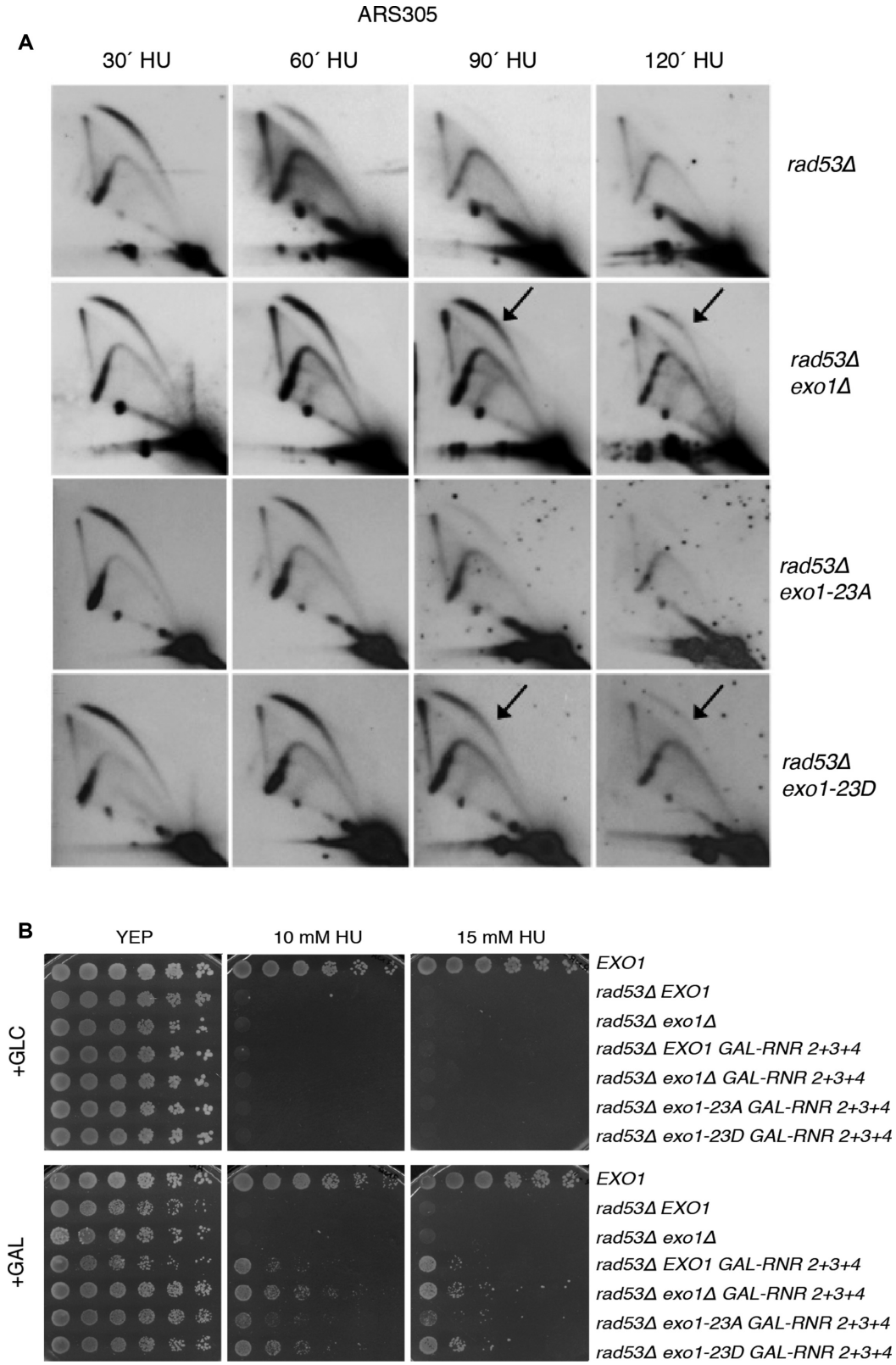

Figure 4. *exo1–23D* phospho-mimic mutant rescues fork collapse in a *rad53Δ* mutants in the presence of replicative stress. (**A**) Two-dimensional gel electrophoresis analysis of DNA replication intermediates at the ARS305 origin from *exo1–23A/23D* mutants and *exo1Δ* mutant in a *rad53Δ* background. Cells were synchronized with α-factor and released into YPD in the presence of 0.2M HU for 2 h. Samples were taken every 30 min, DNA was purified, and DNA replication intermediates were analysed by 2D gel electrophoresis. The arrows point to replication bubbles that persist after 90 min of nucleotide depletion, indicative of fork stability. (**B**) The 1:5 serial dilutions of the indicated strains grown in YEP-raffinose were spotted in YEP medium containing either glucose (GLC) or galactose (GAL) supplemented with 10 mM, 15 mM of HU or no drug and incubated 2–3 days at 30°C.

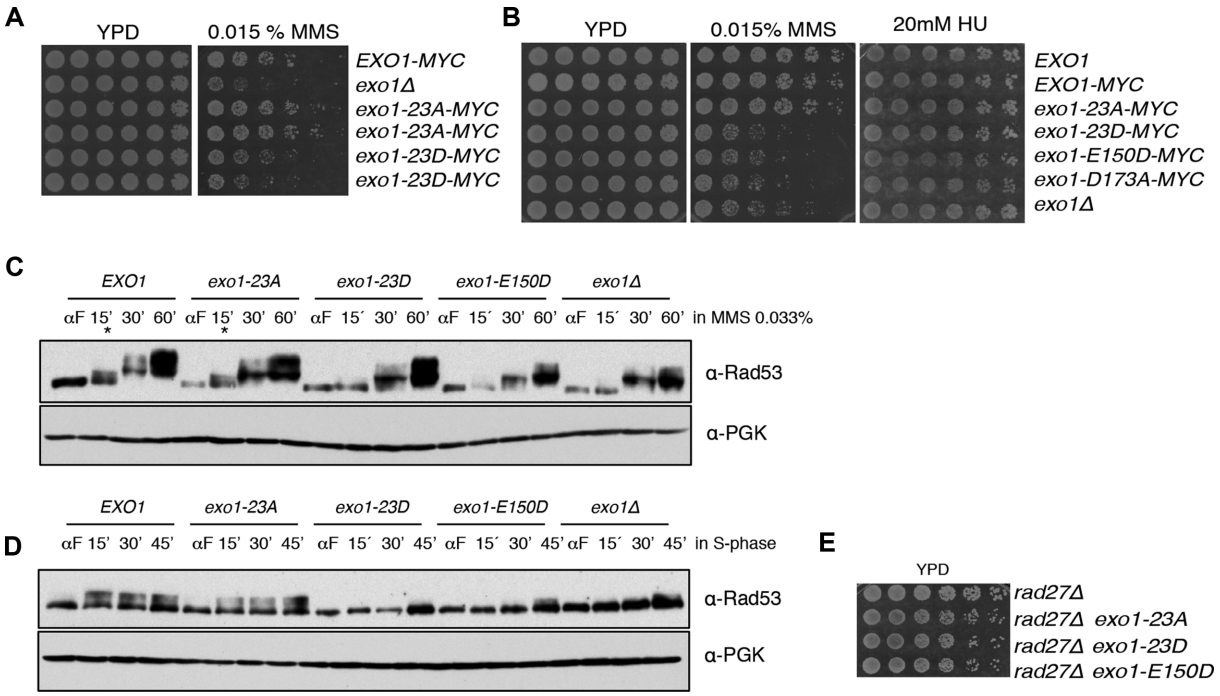

Figure 5. *exo1–23D* phospho-mimic mutant shows an exonuclease deficient and flap-nuclease proficient phenotype. (**A** and **B**) The 1:5 serial dilutions of the indicated strains were tested for sensitivity to 0.015% MMS in YPD plates by using a drop assay. (**C**) Analysis of Rad53 phosphorylation during S phase in the presence of MMS in the indicated strains. Cells were synchronized in G1 and released into S phase in YEPD medium containing 0.033% MMS. Rad53 and PGK were detected by immunoblot with α-Rad53 and α-PGK antibodies respectively. An * has been used to mark the 15 min time point where Rad53 phosphorylation is detected in *EXO1*$^{+}$ and *exo1–23A* strains, but not in the others. (**D**) Analysis of RAD53 phosphorylation in the indicated strains. Cells were arrested in G1, treated with 0,08% MMS for 30 min and then released into S phase in YEPD medium. Rad53 and PGK were detected as described in (B). (**E**) Drop assay of the indicated strains in YPD plates as described in (A).

but the *exo1-E150D* and *exo1–23D* strains exhibited a further delay in Rad53 phosphorylation, which started to be weakly detectable at 45 min (Figure 5D).

These results indicated that Exo1-mediated resection is affected in *exo1–23D* and *exo1-E150D* mutants, but not in *exo1–23A*, supporting that the phospho-mimic allele *exo1–23D* is also 5′-3′ exonuclease defective.

Regarding flap-endonuclease activity, its requirement to survive in the absence of *RAD27* has been previously demonstrated by showing that an *exo1-E150D* mutant is viable in combination with *RAD27* deletion, but an *exo1-D173A* is synthetic lethal with *RAD27* deletion (55). We compared the genetic interactions between these nuclease deficient mutants with *RAD27* and the one exhibited by the phospho-mimic *exo1–23D* allele. Our results recapitulated that an *exo1-D173A rad27Δ* strain was unviable, like the *exo1Δ rad27Δ* one, but the *exo1-E150D rad27Δ* strain was viable (Supplementary Figure S3A). Interestingly, it exhibited similar growth than an *exo1–23D rad27Δ* strain, judging by the similar colony size reached in YEPD plates (Figure 5E), arguing that the *exo1–23D* allele maintains flap-endonuclease activity to promote survival in the absence of *RAD27*.

Replication fork collapse in *rad53* mutants is independent of Exo1-flap endonuclease activity

Next, we reasoned that if Exo1–23D maintains flap-endonuclease activity, but replication forks were stable in *rad53 exo1–23D* mutants in HU, Exo1 flap-endonuclease activity might not be involved in fork degradation and we could take advantage of the different catalytic activities of the nuclease mutants *exo1-D173A* and *exo1-E150D* to determine the nuclease activity involved in fork collapse in *rad53* mutants experiencing replication stress. Thus, we synchronized *rad53Δ exo1Δ, rad53Δ exo1-E150D* and *rad53Δ exo1-D173A* cells in G1 and released them in fresh media in the presence of 0.2M HU. We monitored DNA content by flow cytometry along the experiment (Supplementary Figure S7A) and performed 2D gel analysis of DNA replication intermediates on ARS305. We observed that in the *rad53Δ exo1-D173A* cells the replication bubbles and large Ys were stable through the 2 h of analysis (Figure 6 and Supplementary Figure S7B). These cells are catalytically inactive for both dsDNA 5′-3′ exonuclease and flap-endonuclease activities and, therefore, the stability of replication forks in this strain evidences that fork collapse is linked to Exo1 nuclease activity. Remarkably, *rad53Δ exo1-E150D* cells were equally proficient in preserving fork integrity despite harbouring flap-endonuclease activity, strongly supporting that flap-endonuclease activity is not involved in fork collapse of *rad53* mutants in the presence of replicative stress. These results point out for the first time the enzymatic activity responsible of the collapse of replication forks in *rad53* mutants, which would be relevant to understand the substrates and DNA transitions formed in replication forks after long stalling in the absence of a functional checkpoint.

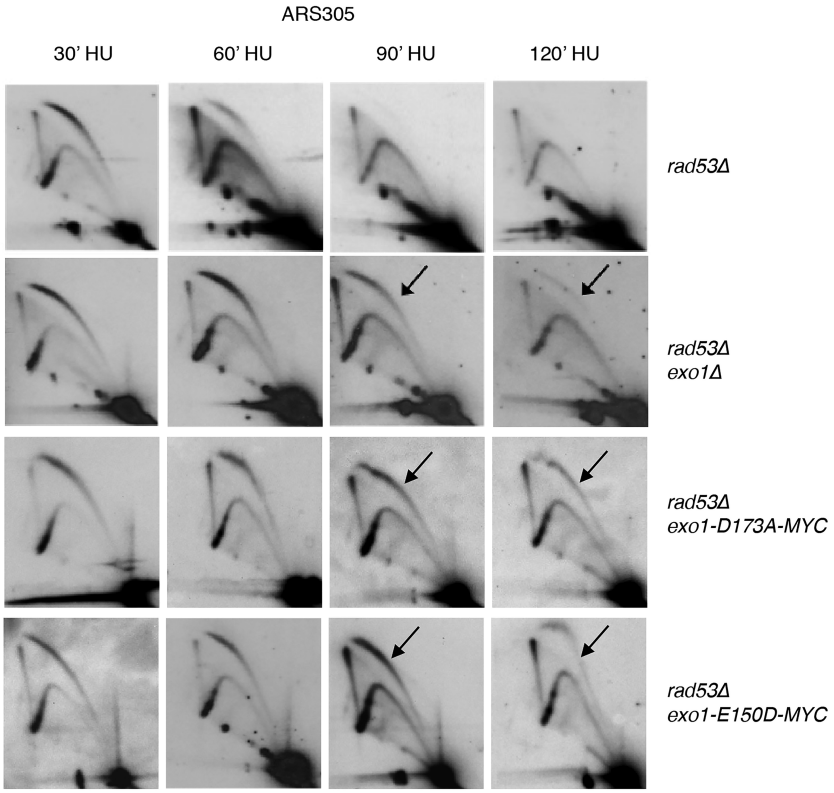

Figure 6. Fork collapse in *rad53Δ* mutants is linked to Exo1′s exonuclease activity but not to its flap-endonuclease activity. Two-dimensional gel electrophoresis analysis of DNA replication intermediates from *exo1-E150D rad53Δ*, *exo1-D173A rad53Δ* and *exo1Δ rad53Δ* mutants were performed as described in Figure 4.

The 14-3-3 proteins are not required for maintaining fork stability in *rad53 exo1-23D* mutants

14-3-3 proteins have been proposed to regulate Exo1 phosphorylation and, in turn, fork processing and stability (48). It was therefore possible that instead of an irrelevant role of Exo1 flap-endonuclease activity in fork degradation, the interaction between the 14-3-3 proteins and the *exo1–23D* version of Exo1, which mimic phosphorylation (Figure 3 B–D), would limit its flap-activity on replication fork substrates and explain the suppression of fork collapse observed in *rad53Δ exo1–23D* mutants in HU. We have confirmed the interaction between Exo1 and Bmh1, the major isoform of the 14-3-3 proteins, and shown that it is specifically detected in HU-treated cells during S phase (Figure 7A). Moreover, we have shown that the Exo1/Bmh1 interaction is largely dependent on Rad53 (Figure 7A), but whether Rad53-dependent Exo1 phosphorylation is important for the 14-3-3 protein binding is not known. To explore this possibility, Bmh1-bound Exo1 was resolved in Phos-tag gels, and we observed phosphorylated forms in the co-immunoprecipitated Exo1 fraction (Figure 7B), indicating that 14-3-3 proteins interact with phosphorylated Exo1. Interestingly, this interaction is preserved in the Exo1–23D phospho-mimic version (Figure 7C), supporting that it behaves like a functional phospho-mimic. On the contrary, the interaction was not detected with the phospho-null Exo1–23A version, strongly arguing that Exo1 binding to 14-3-3 proteins is phospho-dependent.

To examine whether the suppression of fork collapse observed in the *rad53Δ exo1–23D* strain was mediated by the 14-3-3 proteins, we analysed the stability of replication forks in a *rad53Δ exo1–23D bmh2Δ bmh1–266* strain, in which all the 14-3-3 proteins are not functional. When replication intermediates were analysed by 2D gel under conditions of nucleotide depletion, we observed that fork integrity was maintained in both the *rad53Δ exo1–23D* and the *rad53Δ exo1–23D bmh2Δ bmh1–266* strains (Figure 7D and Supplementary Figure S8) and, therefore, the 14-3-3 proteins are not required to maintain fork stability in these mutants. A plausible explanation of our results is that *exo1–23D* suppresses fork collapse in *rad53* mutants because it is defective in exonuclease activity, which as shown above (Figure 6) is likely responsible of the degradation of replication forks.

exo1-23D phospho-mimic mutants are exonuclease-deficient

Until now, all the *in vivo* phenotypes analysed indicated that the *exo1–23D* allele appears to be exonuclease deficient and flap-endonuclease proficient to some extent, whereas the *exo1–23A* seems not affected in activity. To test this prediction, we investigated the *in vitro* nuclease activities of Exo1–23A and Exo1–23D phospho-mutants, in parallel with previously biochemically characterized Exo1, Exo1-E150D and Exo1-D173A proteins (55). In each case, MYC-tagged proteins were immunoprecipitated from S-phase cells, and the nuclease activity tested on two different synthetic sub-

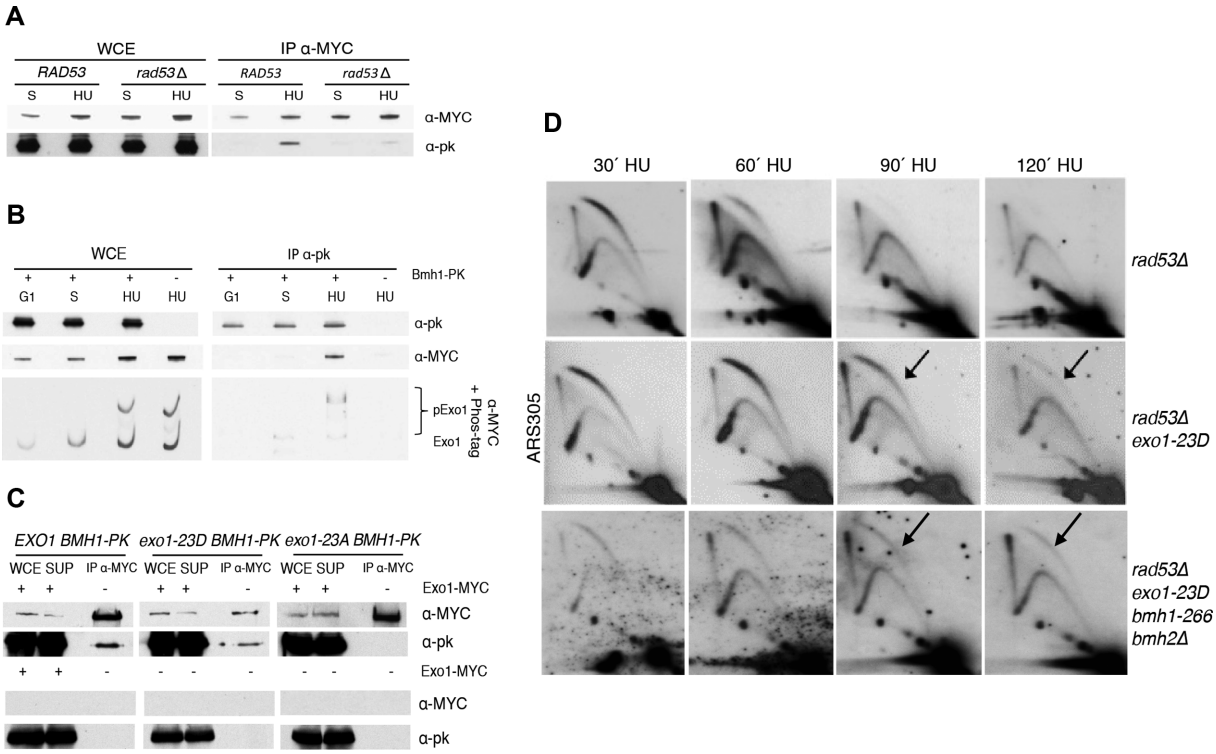

Figure 7. Suppression of fork collapse in *exo1–23D rad53Δ* mutants is independent of the 14-3-3 proteins. (**A**) Analysis of Bmh1-PK and Exo1-MYC interaction in *EXO1-MYC BMH1-PK and EXO1-MYC BMH1-PK rad53Δ* strains. G1-blocked cells were released into YPD medium containing or not 0.2M HU for 90 min. Cells were harvested and proteins were pulled down with α-MYC antibody, and a fraction of the Whole Cell Extract (WCE), and the co-immunoprecipitated proteins (IP) are shown in the immunoblot. Exo1-MYC was detected with α-MYC antibody and Bmh1-PK with α-PK antibody. (**B**) Co-immunoprecipitation assay of Exo1-MYC as described in (A). Proteins were pulled down with α-PK antibody. Analysis of Phostag-SDS page from WCE and IP proteins are shown in the lower panel. (**C**) Immunoblot of a co-immunoprecipitation assay of an *EXO1-MYC BMH1-PK,* an *exo1–23D-MYC BMH1-PK* and an *exo1–23A-MYC BMH1-PK* strains in HU as in (A) is shown in the upper panels. Strains that lacked MYC-tagged Exo1 were used for the co-immunoprecipitation assay shown in the lower panels (*EXO1*$^{+}$ *BMH1-PK*, *exo1–23D BMH1-PK* and *exo1–23A BMH1-PK*). A fraction of the supernatant (Sup.) is also shown in the immunoblot. (**D**) Analysis of replication intermediates by 2D gel electrophoresis at the ARS305 in *rad53Δ exo1–23D bmh2Δ bmh1–266* strains in the presence of 0.2 M HU. The graphs show the quantification analysis of replication bubbles.

strates that allow specific detection of 5′ flap-endonuclease (splayed arm, Figure 8A) or 5′-3′ exonuclease activitiy (5′-recessed dsDNA, Figure 8B).

In the assay with the splayed arm, the endonucleolytic processing of the structure would result in the appearance of an 11-nt labelled product. As shown in Figure 8A, all Exo1 variants displayed endonuclease activity, as judged by the conversion of the full-length oligonucleotide into the smaller product, except in those reactions performed with an untagged strain or with IP-Exo1-D173A. When the enzymatic activity of these Exo1 variants was assayed on a 5′recessed dsDNA substrate, wild-type Exo1 and Exo1–23A exhibited 5′-3′ exonuclease activity whereas the Exo1–23D mutant was clearly deficient for this activity (Figure 8B), supporting our initial premise. Furthermore, Exo1–23D catalytic activity pattern mirrors the one observed in Exo1-E150D, whereas Exo1-D173A lacked both endonuclease and 5′-3′ exonuclease activities as previously reported (55).

These results confirm that Exo1–23A was proficient in both 5′ flap-endonuclease and 5′-3′ exonuclease activities, whereas Exo1–23D displayed endonuclease activity, but a marked deficiency in 5′-3′ exonuclease activity. These results are in agreement with the *in vivo* phenotypes of the Exo1 phospho-mutant strains and strongly suggest that phosphorylation has a direct inhibitory effect on the 5′-3′ exonuclease activity of Exo1.

DISCUSSION

There are differences in the regulation of replication forks in the presence of dNTP depletion or DNA damage. In both situations, Exo1 negative regulation is required to preserve fork stability, but whereas in MMS this inhibition restores replication fork progression (41), in HU it does not (29,41). We wondered whether this could be due to a different Rad53-dependent regulation of Exo1 in each circumstance. Rad53 is indeed differently phosphorylated in response to different genotoxic stresses (65–67) and distinct phosphatases are also involved in the removal of phosphorylation in each situation (68–71). However, whether these differences in Rad53 regulation depending on the nature of the DNA lesion, are also extrapolated to downstream events of the checkpoint response such as the post-translational modifications of checkpoint targets, is not known.

Although a precise proteomic approach will be necessary to determine whether the same phosphorylation residues are phosphorylated *in vivo* after DNA damage or dNTP de-

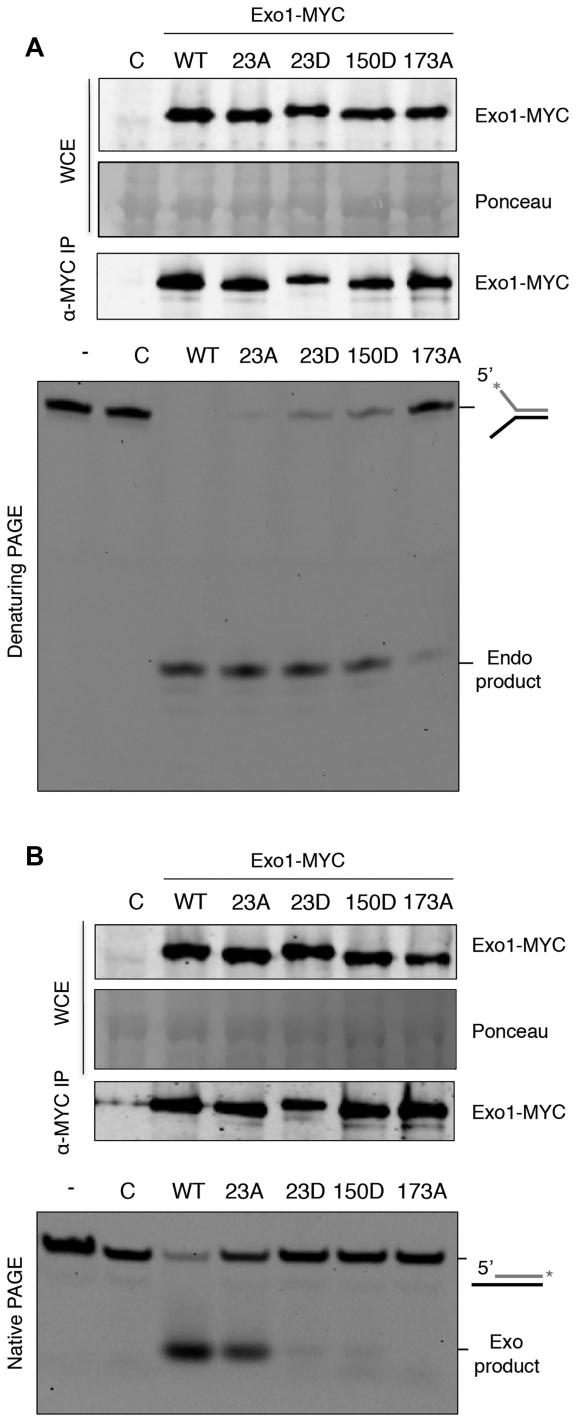

Figure 8. *In vitro* nuclease activity of Exo1 variants. (**A**) Extracts from *EXO1-MYC, exo1–23A-MYC, exo1–23D-MYC*, *exo1-E150D-MYC* and *exo1-D173A-MYC* strains were prepared from S-phase cells and Exo1-MYC variants were detected in the whole cell extracts (WCE) and immunoprecipitates (MYC-IP) by western blotting (upper panels). The analysis of 5′ flap-endonuclease activity of the immunoprecipitated Exo1 variants using a 5′-6FAM-labelled splayed arm is shown in the lower panel. 'C', control reaction using immunoprecipitates from an untagged strain; '-', reaction without extract. The 11-nt product resulting from the endonucleolytic cleavage of the substrate is indicated. (**B**) Exonuclease activity in immunoprecipitates from the same strains as in (A) was assessed using a 5′-recessed double-stranded DNA with 3′-6FAM-labelling. The product of 5′-3′ exonuclease activity is indicated.

pletion, our data suggests that there is not a clear distinct Exo1 regulation after MMS or HU treatment, as in both situations Exo1 phosphorylation is Dun1-independent and Rad53-dependent, and a very similar and reproducible pattern of phosphorylated bands was observed in the different experiments performed along the study (Figure 1B, Supplementary Figure S1C, Figures 2A-B and 3B-C). Moreover, previous results (46–48,72) and ours (this work) argue that phosphorylation sites are redundant, probably to guarantee the transduction of the checkpoint signal through the cascade in the face of impediments that might block or occupy some of the prevalent phosphorylation sites. This notion is supported by the fact that several Exo1 phosphorylation residues have been found by different approaches and conditions, which probably represent the preferential ones, but other sites identified in different studies do not overlap (46–48); (this work). In addition, eliminating a subset of phosphorylation sites was not sufficient to abolish the phosphorylation shift of Exo1 *in vivo* (49) (and Supplementary Figure S2B of this work), or to confer a significant phenotype to the resulting strains carrying the modified versions of the protein, indicating that the regulation of Exo1 is achieved through multiple phosphorylations. Similarly, a multitude of phosphorylation sites have been estimated in human EXO1 (50,53,73), and mutations in specific residues like Ser 714 identified as a phosphorylation site *in vivo*, was not sufficient to abrogate checkpoint-dependent regulation or to avoid EXO1 degradation after replicative stress (50). Other Rad53 substrates are also hyper-phosphorylated (74), indicating that phosphorylation at multiple sites is a common mechanism to transduce the signal of the S phase checkpoint kinases to their targets.

Regarding Exo1 as an important factor involved in fork stability (29,41), and knowing that Exo1 is phosphorylated in a checkpoint dependent manner (46–49), an important issue was to investigate the correlation between Exo1 phosphorylation and fork stability. Our results have shown that the *exo1–23D* mutant, that mimics constitutive phosphorylation (Figure 3B and C), rescues fork collapse in *rad53Δ* mutants treated with HU (Figure 4A) as efficiently as *EXO1* deletion, arguing that the stability of replication forks is achieved mainly through Exo1 phosphorylation. By this, we mean that replication forks of *rad53Δ exo1Δ* and *rad53Δ exo1–23D* strains, when analysed by standard 2D gels, show stable bubbles and large Y molecules along the HU treatment (Figure 4A and Supplementary Figure S4B), indicative of suppression of fork collapse as previously reported (29). Our results do not exclude that other unusual replication intermediates that are not detectable by conventional 2D gels may be transitory at replication forks under these conditions. Nevertheless, the important point is that the phospho-mimic *exo1–23D* allele parallels suppression of fork collapse in *rad53* mutants as the absence of Exo1 does. What makes Exo1 the more relevant nuclease involved in fork degradation, despite being non-essential and redundant with other proteins with the same catalytic activities remains to be elucidated.

Remarkably, we observed a clear correlation between suppression of fork collapse and increased viability in the presence of HU in the phospho-mimic mutants (Figure 4B). As previously reported, cell viability in the presence

of dNTP depletion requires stable replication forks, but not only, and other events, like RNR induction, are additionally necessary to promote replication resumption and survival under these conditions (43). Our results showed that the *exo1–23D* allele and *EXO1* deletion confers similar HU-resistance in *rad53* mutants upon RNR induction, suggesting that in both cases replication forks must be similarly competent to restart and finish replication to some extent (43), which is essential to support viability. This fact excludes that other Exo1 regulatory mechanism distinct than phosphorylation is required for the competence to restart stalled forks when appropriate conditions are restored.

Thus, the regulation of replication forks after replicative stress is a complex task and involves different mechanisms. Rad53-dependent phosphorylation of Exo1 preserves fork stability, Rad53-dependent RNR induction promotes fork restart (43,75), and several factors such as the DNA helicases Rrm3 and Pif1 (25), BLM helicases (76), the nucleases Dna2, Sae2 and Mus81 (45–46,50,77–80), and the DNA polymerase α–primase complex (81,82) have been proposed to also contribute to control fork restart, fork reversal or coupling between leading and lagging strands synthesis in yeast and human cells. Although how the S phase checkpoint does coordinate all these factors to promote fork stability and restart after replication blockage has not been elucidated yet.

Rescue of fork collapse was also recapitulated in the absence of Exo1 nuclease activity, since the nuclease-dead (ND) mutant *exo1-D173A* reproduces the suppression of fork collapse (Figure 6), indicating that fork collapse was dependent on its nuclease activity. This result also highlights that merely the presence of Exo1 is not deleterious for the integrity of replication forks and discard a possible structural role of Exo1 on fork stability. Interestingly, in both nuclease deficient mutants (*rad53Δ exo1-D173A* and *rad53Δ exo1-E150D*) replication forks are stabilized, despite the fact that *exo1-E150D* maintains substantial flap-endonuclease activity (55), arguing that fork collapse in the absence of a functional checkpoint is specifically dependent on the exonuclease activity of Exo1. We cannot rule out the possibility that the residual flap-endonuclease activity of *exo1-E150D* could be insufficient to degrade replication forks. However, the flap-endonuclease activity of an *exo1-E150D* strain is sufficient to keep cells alive, with a good fitness in the absence of *RAD27* (Figure 5E and Supplementary Figure S3A), indicating that it possesses enough flap-endonuclease activity to perform an essential function, being most likely Okazaki fragment processing as it has been suggested (55).

Similarly, the *exo1–23D* strain did not show synthetic lethality with *RAD27* deletion (Figures 3A, 5E and Supplementary Figure S3), pointing out two important facts: first, that Exo1–23D also conserves flap-endonuclease activity, and second that it is, therefore, a functional protein capable of performing a vital step of DNA replication. However, we cannot exclude that protein function might be affected by these 23 modifications to some extent. This result let us to hypothesize that phosphorylation could have a distinct effect on the exonuclease and flap-activities of Exo1. Several *in vivo* phenotypes exhibited by *exo1–23D* were indicative of a defective 5′-3′exonuclease activity, such as similar sensitivity to MMS as an *exo1Δ* or an *exo1-ND* strain (Figure 5B) (39) and a similar delay in Rad53 phosphorylation (Figure 5C and D) (49). In agreement with this idea, the *in vitro* nuclease assays demonstrated that the Exo1–23D phospho-mimic variant possessed endonuclease activity but was clearly deficient for 5′-3′exonuclease activity (Figure 8). Thus, we propose that checkpoint-dependent phosphorylation of Exo1 specifically inhibits the exonuclease activity of Exo1, responsible for the collapse of stalled forks.

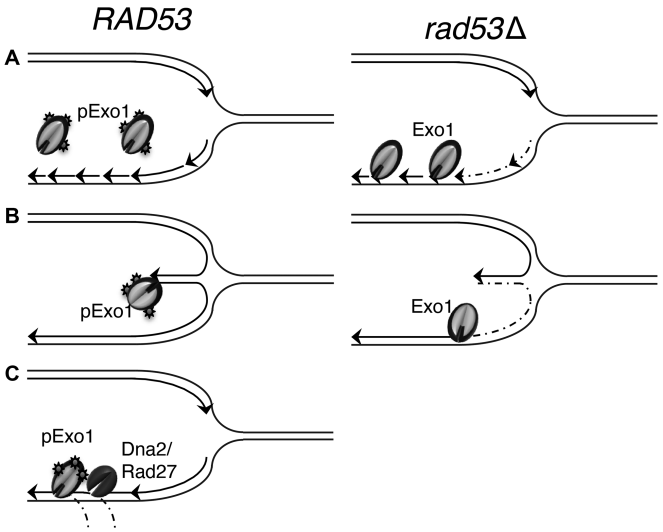

Figure 9. Scheme of potential Exo1′s substrates that may be available during replicative stress. (**A**) Gapped molecules at nascent strands. (**B**) Reversed forks. (**C**) Long flaps, which could be also processed by Dna2 and/or Rad27.

One possibility to explain this regulation would be that the 5′-3′exonuclease activity of Exo1 is specifically detrimental to the integrity of replication forks after replicative stress because it acts on several key substrates generated or exposed in checkpoint mutants after fork stalling (Figure 9). One of these substrates is probably the 5′ end of gaps present in the nascent strands of HU-treated *rad53* mutant cells (Figure 9A), possibly originated after uncoupling between DNA unwinding by replicative helicases and DNA synthesis or due to defects in leading or lagging strand synthesis (32). Resection of the gap ends by Exo1 could explain the accumulation of single-stranded regions found at stalled forks in *rad53* mutants in HU (29), which can possibly promote fork reversal. Reversed forks are in fact, other potential substrate for the 5′-3′ exonuclease activity of Exo1 (Figure 9B), which have been also observed in *rad53* cells upon HU treatment (26,29). Reversed forks are DNA structures represented by four-branched molecules, which can arise from re-annealing of the parental strands and extrusion or degradation of the nascent strands, although the precise origin of these unusual structures and their role in fork stability and restart is not totally clear (32). Which seems clear is that Exo1 5′-3′exonuclease activity participates in the nucleolytic processing of these DNA substrates, because elimination of Exo1 counteracts the accumulation of ssDNA gaps at nascent strands and increases the rate of fork reversal (29). A similar role for human EXO1 in the resection of reversed forks has been described. In this system, it has been pro-

posed that BRCA2 protects the regressed arms of reversed forks from nucleolytic degradation by the CtIP, MRE11 and EXO1 nucleases (83).

Besides a plausible deleterious effect of unscheduled 5′-3′ exonuclease activity on replication forks, the 5′ flap-endonuclease activity of Exo1 might be favourable to cope with some toxic DNA structure generated at arrested replication forks in checkpoint mutants. In fact, the formation of long 5′ flaps at the lagging strand of uncoupled replication forks have been proposed (84), which would be processed by flap-endonucleases such as Exo1 to avoid the formation of pathological structures at forks (Figure 9C). Although during unperturbed replication, other flap-endonucleases like Rad27 and Dna2 are mainly responsible of the processing of long flaps generated during Okazaki fragment processing (85), in conditions that induce fork stalling the complexity of the discontinuous synthesis of the lagging strand would require additional mechanisms to preserve fork structure. A high number of Okazaki fragments must be processed per replication cycle (86), and in conditions that induce fork stalling and strand displacement, the concerted action of several flap-endonucleases such as Rad27-Dna2-Exo1 might represent an advantageous backup mechanism to guarantee proper processing of thousands of unusually long flaps that otherwise would led to the generation of toxic DNA structures at replication forks (Figure 9C). In fact, the contribution of several flap-endonucleases like Exo1 and Dna2 in counteracting the formation of unusual DNA replication intermediates in checkpoint defective cells exposed to replication stress has been proposed (45). Accumulation of long ssDNA flaps have been observed by electron microscopy in the absence of Dna2 (87); however, these structures have not been detected at stalled replication forks in *rad53* mutants in the absence of Exo1. Therefore, the Exo1 contribution to long ssDNA flaps processing is currently uncertain.

It is worth noting that although other nucleases might help to eliminate aberrant replication intermediates, which can be beneficial under some circumstances, our results strongly argue that Rad53-dependent Exo1 regulation, through direct inhibition of its exonuclease activity, is enough to maintain stable replication forks after dNTP depletion in budding yeast.

Besides nuclease activity, Exo1 phosphorylation could also regulate the protein's stability, interactions and/or cellular localization. In relation with protein stability, it has been previously shown that in response to replicative stress, ATR-dependent phosphorylation of human EXO1 induces polyubiquitylation and proteasome-mediated degradation (50,51), although this regulatory mechanism does not seem to operate in budding yeast. In this case, Exo1 protein levels are not affected by phosphorylation in response to HU ((48), Figure 1B and Supplementary Figure S1C) or MMS (Figure 1B and Supplementary Figure S1C). Moreover, the level of expression of the phospho-null Exo1–23A or phospho-mimic Exo1–23D versions generated in this study were not substantially different from the wild-type Exo1 protein (Supplementary Figure S6B). It is worth mentioning that in our experiments, Exo1 protein levels remain constant also during an unperturbed cell cycle (Figure 1A and Supplementary Figure S1B), although a recent study has reported that Exo1 protein levels fluctuate along the cell cycle independently of Rad53 (49). These differences might be due to a different experimental set-up, as in their experiments, α-factor was re-added during S phase.

Regarding to the importance of protein interactions in Exo1 regulation, a conserved EXO1/14-3-3 proteins interaction from yeast to mammalian cells has been described (48,88). In yeast, this interaction depends on an active checkpoint, while human EXO1 constitutively interacts with the 14-3-3 proteins, through a binding domain that is not present in yeast Exo1 (89). In fact, while the nuclease domain of EXO1 is highly conserved (90), its C-terminal region, which mediates interaction with other proteins, is not (61). The interaction between human EXO1 and the 14-3-3 proteins suppresses EXO1 recruitment to damaged sites and avoid overresection by reducing its association with PCNA (89,91–92). However, this association has not been described in yeast and the role of the EXO1/14-3-3 proteins interaction could be very different in yeast and human cells. Also distinct from yeast Exo1, the C-terminus of human EXO1 is phosphorylated by CDKs in the S/G2 phases of the cell cycle, which regulates EXO1 recruitment to DSBs.

14-3-3 proteins can bind phosphorylated proteins (93), and, in yeast, they have been proposed to promote fork stability and progression by regulating the phosphorylation status of Exo1 (48,88), although it was not known whether 14-3-3 proteins bind phosphorylated or unphosphorylated Exo1. We have shown here that Bmh1 interacts with phosphorylated wild-type Exo1 protein (Figure 7B), and this interaction is preserved with Exo1–23D (Figure 7C), indicating that it behaves like a functional phospho-mimic version. Remarkably, the Exo1/Bmh1 interaction is Rad53-dependent (Figure 7A) and it is not detected in the *exo1–23A* phospho-null mutant (Figure 7C), indicating that the binding of 14-3-3 proteins to Exo1 is phospho-dependent. These results may be important to understand the nature of the binding of 14-3-3 proteins to checkpoint targets like Exo1. Our results indicated that fork stability is maintained in *rad53exo1–23D* mutants in HU in the absence of functional 14-3-3 proteins (Figure 7D). Therefore, the 14-3-3 proteins may help control Exo1 together with checkpoint-dependent phosphorylation, perhaps by inducing or supporting Exo1 hyper-phosphorylation, but once established this stage, they seem dispensable to preserve fork stability. It has been recently proposed that the 14-3-3 proteins regulate Exo1 cellular localization (94). However, this regulation does not require Rad53-dependent phosphorylation. Therefore, at the present time, the biological meaning of the Exo1/14-3-3 interaction in the frame of the checkpoint response to replication stress is still unclear.

A defective Exo1 regulation has a great impact in the stability of replication forks under replicative stress leading to fork collapse and the inability to restart damaged forks, which can result in double-strand breaks, genome rearrangements and cell death. All these events threaten genome stability and can let to cellular transformation. In fact, increased levels of EXO1 are detrimental and lead to genomic instability (95), and deregulation of EXO1 protein levels in tumours is commonly reported (96,97). Therefore, deciphering how the S phase checkpoint restrains Exo1 activity can be relevant to develop cancer therapies.

SUPPLEMENTARY DATA

Supplementary Data are available at NAR Online.

ACKNOWLEDGEMENTS

We thank John Diffley for providing the JDI48 antibody and reagents, Rodrigo Bermejo for providing strains and plasmids, Karim Labib for providing strains and help with immunoprecipitations experiments, Mikel Liskay for providing the YIp-exo1-D173A and YIp-exo1-E150D plasmids. We thank Rodrigo Bermejo for critically reading the manuscript.

FUNDING

Spanish Ministry of Economy and Competitiveness (MINECO) [FEDER-BFU2013-45182-P to C.M.C., M.S.]; University of Salamanca [KA6H/463AC01 to M.S.]; MINECO, AEI, Xunta de Galicia and FEDER [RYC-2012-10835, BFU2016-78121-P, ED431F-2016/019, ED431B-2016/016 to M.G.B.]; Junta de Castilla y León (JCyL), Program 'Escalera de Excelencia' [FEDER-CLU-2017-03]; JCyL Pre-doctoral Fellowship (to A.B.); MINECO Pre-Doctoral Fellowship (to E.C.M.); Xunta de Galicia Pre-doctoral Fellowship (ED481A-2018/041 to R.C.). Funding for open access charge: University of Salamanca.
Conflict of interest statement. None declared.

REFERENCES

1. Paulovich,A.G. and Hartwell,L.H. (1995) A checkpoint regulates the rate of progression through S phase in S. cerevisiae in response to DNA damage. *Cell*, **82**, 841–847.
2. Zhou,B.B. and Elledge,S.J. (2000) The DNA damage response: putting checkpoints in perspective. *Nature*, **408**, 433–439.
3. Yazinski,S.A. and Zou,L. (2016) Functions, regulation, and therapeutic implications of the ATR checkpoint pathway. *Annu. Rev. Genet.*, **50**, 155–173.
4. Neelsen,K.J., Zanini,I.M., Herrador,R. and Lopes,M. (2013) Oncogenes induce genotoxic stress by mitotic processing of unusual replication intermediates. *J. Cell Biol.*, **200**, 699–708.
5. Hartwell,L.H. and Kastan,M.B. (1994) Cell cycle control and cancer. *Science*, **266**, 1821–1828.
6. Kolodner,R.D., Putnam,C.D. and Myung,K. (2002) Maintenance of genome stability in Saccharomyces cerevisiae. *Science*, **297**, 552–557.
7. Nyberg,K.A., Michelson,R.J., Putnam,C.W. and Weinert,T.A. (2002) Toward maintaining the genome: DNA damage and replication checkpoints. *Annu. Rev. Genet.*, **36**, 617–656.
8. Bartkova,J., Horejsi,Z., Koed,K., Kramer,A., Tort,F., Zieger,K., Guldberg,P., Sehested,M., Nesland,J.M., Lukas,C. *et al.* (2005) DNA damage response as a candidate anti-cancer barrier in early human tumorigenesis. *Nature*, **434**, 864–870.
9. Gorgoulis,V.G., Vassiliou,L.V., Karakaidos,P., Zacharatos,P., Kotsinas,A., Liloglou,T., Venere,M., Ditullio,R.A. Jr, Kastrinakis,N.G., Levy,B. *et al.* (2005) Activation of the DNA damage checkpoint and genomic instability in human precancerous lesions. *Nature*, **434**, 907–913.
10. Barlow,C., Hirotsune,S., Paylor,R., Liyanage,M., Eckhaus,M., Collins,F., Shiloh,Y., Crawley,J.N., Ried,T., Tagle,D. *et al.* (1996) Atm-deficient mice: a paradigm of ataxia telangiectasia. *Cell*, **86**, 159–171.
11. Elson,A., Wang,Y., Daugherty,C.J., Morton,C.C., Zhou,F., Campos-Torres,J. and Leder,P. (1996) Pleiotropic defects in ataxia-telangiectasia protein-deficient mice. *Proc. Natl. Acad. Sci. U.S.A.*, **93**, 13084–13089.
12. Xu,Y. and Baltimore,D. (1996) Dual roles of ATM in the cellular response to radiation and in cell growth control. *Genes Dev.*, **10**, 2401–2410.
13. al-Khodairy,F., Fotou,E., Sheldrick,K.S., Griffiths,D.J., Lehmann,A.R. and Carr,A.M. (1994) Identification and characterization of new elements involved in checkpoint and feedback controls in fission yeast. *Mol. Biol. Cell*, **5**, 147–160.
14. Murakami,H. and Okayama,H. (1995) A kinase from fission yeast responsible for blocking mitosis in S phase. *Nature*, **374**, 817–819.
15. Tourriere,H. and Pasero,P. (2007) Maintenance of fork integrity at damaged DNA and natural pause sites. *DNA Repair (Amst.)*, **6**, 900–913.
16. Branzei,D. and Foiani,M. (2006) The Rad53 signal transduction pathway: replication fork stabilization, DNA repair, and adaptation. *Exp. Cell Res.*, **312**, 2654–2659.
17. Zhou,Z. and Elledge,S.J. (1993) DUN1 encodes a protein kinase that controls the DNA damage response in yeast. *Cell*, **75**, 1119–1127.
18. Allen,J.B., Zhou,Z., Siede,W., Friedberg,E.C. and Elledge,S.J. (1994) The SAD1/RAD53 protein kinase controls multiple checkpoints and DNA damage-induced transcription in yeast. *Genes Dev.*, **8**, 2401–2415.
19. Santocanale,C. and Diffley,J.F. (1998) A Mec1- and Rad53-dependent checkpoint controls late-firing origins of DNA replication. *Nature*, **395**, 615–618.
20. Shirahige,K., Hori,Y., Shiraishi,K., Yamashita,M., Takahashi,K., Obuse,C., Tsurimoto,T. and Yoshikawa,H. (1998) Regulation of DNA-replication origins during cell-cycle progression. *Nature*, **395**, 618–621.
21. Foiani,M., Pellicioli,A., Lopes,M., Lucca,C., Ferrari,M., Liberi,G., Muzi Falconi,M. and Plevani,P. (2000) DNA damage checkpoints and DNA replication controls in Saccharomyces cerevisiae. *Mutat. Res.*, **451**, 187–196.
22. Tercero,J.A., Longhese,M.P. and Diffley,J.F. (2003) A central role for DNA replication forks in checkpoint activation and response. *Mol. Cell*, **11**, 1323–1336.
23. Tercero,J.A. and Diffley,J.F. (2001) Regulation of DNA replication fork progression through damaged DNA by the Mec1/Rad53 checkpoint. *Nature*, **412**, 553–557.
24. Lopes,M., Cotta-Ramusino,C., Pellicioli,A., Liberi,G., Plevani,P., Muzi-Falconi,M., Newlon,C.S. and Foiani,M. (2001) The DNA replication checkpoint response stabilizes stalled replication forks. *Nature*, **412**, 557–561.
25. Rossi,S.E., Ajazi,A., Carotenuto,W., Foiani,M. and Giannattasio,M. (2015) Rad53-Mediated Regulation of Rrm3 and Pif1 DNA helicases contributes to prevention of aberrant fork transitions under replication stress. *Cell Rep.*, **13**, 80–92.
26. Sogo,J.M., Lopes,M. and Foiani,M. (2002) Fork reversal and ssDNA accumulation at stalled replication forks owing to checkpoint defects. *Science*, **297**, 599–602.
27. Lucca,C., Vanoli,F., Cotta-Ramusino,C., Pellicioli,A., Liberi,G., Haber,J. and Foiani,M. (2004) Checkpoint-mediated control of replisome-fork association and signalling in response to replication pausing. *Oncogene*, **23**, 1206–1213.
28. Cobb,J.A., Schleker,T., Rojas,V., Bjergbaek,L., Tercero,J.A. and Gasser,S.M. (2005) Replisome instability, fork collapse, and gross chromosomal rearrangements arise synergistically from Mec1 kinase and RecQ helicase mutations. *Genes Dev.*, **19**, 3055–3069.
29. Cotta-Ramusino,C., Fachinetti,D., Lucca,C., Doksani,Y., Lopes,M., Sogo,J. and Foiani,M. (2005) Exo1 processes stalled replication forks and counteracts fork reversal in checkpoint-defective cells. *Mol. Cell*, **17**, 153–159.
30. De Piccoli,G., Katou,Y., Itoh,T., Nakato,R., Shirahige,K. and Labib,K. (2012) Replisome stability at defective DNA replication forks is independent of S phase checkpoint kinases. *Mol. Cell*, **45**, 696–704.
31. Dungrawala,H., Rose,K.L., Bhat,K.P., Mohni,K.N., Glick,G.G., Couch,F.B. and Cortez,D. (2015) The replication checkpoint prevents two types of fork collapse without regulating replisome stability. *Mol. Cell*, **59**, 998–1010.
32. Giannattasio,M. and Branzei,D. (2017) S-phase checkpoint regulations that preserve replication and chromosome integrity upon dNTP depletion. *Cell. Mol. Life Sci.*, **74**, 2361–2380.
33. Dzantiev,L., Constantin,N., Genschel,J., Iyer,R.R., Burgers,P.M. and Modrich,P. (2004) A defined human system that supports bidirectional mismatch-provoked excision. *Mol. Cell*, **15**, 31–41.
34. Fiorentini,P., Huang,K.N., Tishkoff,D.X., Kolodner,R.D. and Symington,L.S. (1997) Exonuclease I of Saccharomyces cerevisiae

functions in mitotic recombination in vivo and in vitro. *Mol. Cell. Biol.*, **17**, 2764–2773.
35. Lewis,L.K., Karthikeyan,G., Westmoreland,J.W. and Resnick,M.A. (2002) Differential suppression of DNA repair deficiencies of Yeast rad50, mre11 and xrs2 mutants by EXO1 and TLC1 (the RNA component of telomerase). *Genetics*, **160**, 49–62.
36. Tishkoff,D.X., Boerger,A.L., Bertrand,P., Filosi,N., Gaida,G.M., Kane,M.F. and Kolodner,R.D. (1997) Identification and characterization of Saccharomyces cerevisiae EXO1, a gene encoding an exonuclease that interacts with MSH2. *Proc. Natl. Acad. Sci. U.S.A.*, **94**, 7487–7492.
37. Jia,X., Weinert,T. and Lydall,D. (2004) Mec1 and Rad53 inhibit formation of single-stranded DNA at telomeres of Saccharomyces cerevisiae cdc13-1 mutants. *Genetics*, **166**, 753–764.
38. Maringele,L. and Lydall,D. (2002) EXO1-dependent single-stranded DNA at telomeres activates subsets of DNA damage and spindle checkpoint pathways in budding yeast yku70Delta mutants. *Genes Dev.*, **16**, 1919–1933.
39. Tsubouchi,H. and Ogawa,H. (2000) Exo1 roles for repair of DNA double-strand breaks and meiotic crossing over in Saccharomyces cerevisiae. *Mol. Biol. Cell*, **11**, 2221–2233.
40. Surtees,J.A. and Alani,E. (2004) Replication factors license exonuclease I in mismatch repair. *Mol. Cell*, **15**, 164–166.
41. Segurado,M. and Diffley,J.F. (2008) Separate roles for the DNA damage checkpoint protein kinases in stabilizing DNA replication forks. *Genes Dev.*, **22**, 1816–1827.
42. Gomez-Gonzalez,B., Patel,H., Early,A. and Diffley,J.F.X. (2018) Rpd3L Contributes to the DNA damage sensitivity of saccharomyces cerevisiae checkpoint mutants. *Genetics*, **211**, 503–513.
43. Morafraile,E.C., Diffley,J.F., Tercero,J.A. and Segurado,M. (2015) Checkpoint-dependent RNR induction promotes fork restart after replicative stress. *Sci. Rep.*, **5**, 7886–7895.
44. Branzei,D. and Foiani,M. (2010) Maintaining genome stability at the replication fork. *Nat. Rev. Mol. Cell Biol.*, **11**, 208–219.
45. Colosio,A., Frattini,C., Pellicano,G., Villa-Hernandez,S. and Bermejo,R. (2016) Nucleolytic processing of aberrant replication intermediates by an Exo1-Dna2-Sae2 axis counteracts fork collapse-driven chromosome instability. *Nucleic Acids Res.*, **44**, 10676–10690.
46. Smolka,M.B., Albuquerque,C.P., Chen,S.H. and Zhou,H. (2007) Proteome-wide identification of in vivo targets of DNA damage checkpoint kinases. *Proc. Natl. Acad. Sci. U.S.A.*, **104**, 10364–10369.
47. Morin,I., Ngo,H.P., Greenall,A., Zubko,M.K., Morrice,N. and Lydall,D. (2008) Checkpoint-dependent phosphorylation of Exo1 modulates the DNA damage response. *EMBO J.*, **27**, 2400–2410.
48. Engels,K., Giannattasio,M., Muzi-Falconi,M., Lopes,M. and Ferrari,S. (2011) 14-3-3 Proteins regulate exonuclease 1-dependent processing of stalled replication forks. *PLos Genet.*, **7**, e1001367.
49. Garcia-Rodriguez,N., Morawska,M., Wong,R.P., Daigaku,Y. and Ulrich,H.D. (2018) Spatial separation between replisome- and template-induced replication stress signaling. *EMBO J.*, **37**, e98369.
50. El-Shemerly,M., Hess,D., Pyakurel,A.K., Moselhy,S. and Ferrari,S. (2008) ATR-dependent pathways control hEXO1 stability in response to stalled forks. *Nucleic Acids Res.*, **36**, 511–519.
51. El-Shemerly,M., Janscak,P., Hess,D., Jiricny,J. and Ferrari,S. (2005) Degradation of human exonuclease 1b upon DNA synthesis inhibition. *Cancer Res.*, **65**, 3604–3609.
52. Tomimatsu,N., Mukherjee,B., Catherine Hardebeck,M., Ilcheva,M., Vanessa Camacho,C., Louise Harris,J., Porteus,M., Llorente,B., Khanna,K.K. and Burma,S. (2014) Phosphorylation of EXO1 by CDKs 1 and 2 regulates DNA end resection and repair pathway choice. *Nat. Commun.*, **5**, 3561–3582.
53. Bologna,S., Altmannova,V., Valtorta,E., Koenig,C., Liberali,P., Gentili,C., Anrather,D., Ammerer,G., Pelkmans,L., Krejci,L. *et al.* (2015) Sumoylation regulates EXO1 stability and processing of DNA damage. *Cell Cycle*, **14**, 2439–2450.
54. Storici,F. and Resnick,M.A. (2006) The delitto perfetto approach to in vivo site-directed mutagenesis and chromosome rearrangements with synthetic oligonucleotides in yeast. *Methods Enzymol.*, **409**, 329–345.
55. Tran,P.T., Erdeniz,N., Dudley,S. and Liskay,R.M. (2002) Characterization of nuclease-dependent functions of Exo1p in Saccharomyces cerevisiae. *DNA Repair (Amst.)*, **1**, 895–912.
56. Foltman,M. and Sanchez-Diaz,A. (2016) Studying protein-protein interactions in budding yeast using co-immunoprecipitation. *Methods Mol. Biol.*, **1369**, 239–256.
57. Rass,U. and West,S. (2006) Synthetic Junctions as Tools to Identify and Characterize Holliday Junction Resolvases. *Methods Enzymol.*, **408**, 485–501.
58. Brewer,B.J., Lockshon,D. and Fangman,W.L. (1992) The arrest of replication forks in the rDNA of yeast occurs independently of transcription. *Cell*, **71**, 267–276.
59. Ivessa,A.S., Zhou,J.Q. and Zakian,V.A. (2000) The Saccharomyces Pif1p DNA helicase and the highly related Rrm3p have opposite effects on replication fork progression in ribosomal DNA. *Cell*, **100**, 479–489.
60. Doerfler,L. and Schmidt,K.H. (2014) Exo1 phosphorylation status controls the hydroxyurea sensitivity of cells lacking the Pol32 subunit of DNA polymerases delta and zeta. *DNA Repair (Amst.)*, **24**, 26–36.
61. Tran,P.T., Erdeniz,N., Symington,L.S. and Liskay,R.M. (2004) EXO1-A multi-tasking eukaryotic nuclease. *DNA Repair (Amst.)*, **3**, 1549–1559.
62. Harder,J. and Follmann,H. (1990) Identification of a free radical and oxygen dependence of ribonucleotide reductase in yeast. *Free Radic. Res. Commun.*, **10**, 281–286.
63. Zou,L. and Elledge,S.J. (2003) Sensing DNA damage through ATRIP recognition of RPA-ssDNA complexes. *Science*, **300**, 1542–1548.
64. Giannattasio,M., Follonier,C., Tourriere,H., Puddu,F., Lazzaro,F., Pasero,P., Lopes,M., Plevani,P. and Muzi-Falconi,M. (2010) Exo1 competes with repair synthesis, converts NER intermediates to long ssDNA gaps, and promotes checkpoint activation. *Mol. Cell*, **40**, 50–62.
65. Pellicioli,A. and Foiani,M. (2005) Signal transduction: how rad53 kinase is activated. *Curr. Biol.*, **15**, R769–R771.
66. Smolka,M.B., Albuquerque,C.P., Chen,S.H., Schmidt,K.H., Wei,X.X., Kolodner,R.D. and Zhou,H. (2005) Dynamic changes in protein-protein interaction and protein phosphorylation probed with amine-reactive isotope tag. *Mol. Cell. Proteomics*, **4**, 1358–1369.
67. Sweeney,F.D., Yang,F., Chi,A., Shabanowitz,J., Hunt,D.F. and Durocher,D. (2005) Saccharomyces cerevisiae Rad9 acts as a Mec1 adaptor to allow Rad53 activation. *Curr. Biol.*, **15**, 1364–1375.
68. Leroy,C., Lee,S.E., Vaze,M.B., Ochsenbein,F., Guerois,R., Haber,J.E. and Marsolier-Kergoat,M.C. (2003) PP2C phosphatases Ptc2 and Ptc3 are required for DNA checkpoint inactivation after a double-strand break. *Mol. Cell*, **11**, 827–835.
69. Travesa,A., Duch,A. and Quintana,D.G. (2008) Distinct phosphatases mediate the deactivation of the DNA damage checkpoint kinase Rad53. *J. Biol. Chem.*, **283**, 17123–17130.
70. Szyjka,S.J., Aparicio,J.G., Viggiani,C.J., Knott,S., Xu,W., Tavare,S. and Aparicio,O.M. (2008) Rad53 regulates replication fork restart after DNA damage in Saccharomyces cerevisiae. *Genes Dev.*, **22**, 1906–1920.
71. Bazzi,M., Mantiero,D., Trovesi,C., Lucchini,G. and Longhese,M.P. (2010) Dephosphorylation of gamma H2A by Glc7/protein phosphatase 1 promotes recovery from inhibition of DNA replication. *Mol. Cell. Biol.*, **30**, 131–145.
72. Albuquerque,C.P., Smolka,M.B., Payne,S.H., Bafna,V., Eng,J. and Zhou,H. (2008) A multidimensional chromatography technology for in-depth phosphoproteome analysis. *Mol. Cell. Proteomics*, **7**, 1389–1396
73. Zheng,X.F., Kalev,P. and Chowdhury,D. (2015) Emerging role of protein phosphatases changes the landscape of phospho-signaling in DNA damage response. *DNA Repair (Amst.)*, **32**, 58–65.
74. Zegerman,P. and Diffley,J.F. (2010) Checkpoint-dependent inhibition of DNA replication initiation by Sld3 and Dbf4 phosphorylation. *Nature*, **467**, 474–478.
75. Lopez-Contreras,A.J., Specks,J., Barlow,J.H., Ambrogio,C., Desler,C., Vikingsson,S., Rodrigo-Perez,S., Green,H., Rasmussen,L.J., Murga,M. *et al.* (2015) Increased Rrm2 gene dosage reduces fragile site breakage and prolongs survival of ATR mutant mice. *Genes Dev.*, **29**, 690–695.
76. Davies,S.L., North,P.S. and Hickson,I.D. (2007) Role for BLM in replication-fork restart and suppression of origin firing after replicative stress. *Nat. Struct. Mol. Biol.*, **14**, 677–679.
77. Kai,M., Boddy,M.N., Russell,P. and Wang,T.S. (2005) Replication checkpoint kinase Cds1 regulates Mus81 to preserve genome integrity during replication stress. *Genes Dev.*, **19**, 919–932.

78. Hu,J., Sun,L., Shen,F., Chen,Y., Hua,Y., Liu,Y., Zhang,M., Hu,Y., Wang,Q., Xu,W. *et al.* (2012) The intra-S phase checkpoint targets Dna2 to prevent stalled replication forks from reversing. *Cell*, **149**, 1221–1232.
79. Froget,B., Blaisonneau,J., Lambert,S. and Baldacci,G. (2008) Cleavage of stalled forks by fission yeast Mus81/Eme1 in absence of DNA replication checkpoint. *Mol. Biol. Cell*, **19**, 445–456.
80. Techer,H., Koundrioukoff,S., Carignon,S., Wilhelm,T., Millot,G.A., Lopez,B.S., Brison,O. and Debatisse,M. (2016) Signaling from Mus81-Eme2-Dependent DNA damage elicited by Chk1 deficiency modulates replication fork speed and origin usage. *Cell Rep.*, **14**, 1114–1127.
81. Marini,F., Pellicioli,A., Paciotti,V., Lucchini,G., Plevani,P., Stern,D.F. and Foiani,M. (1997) A role for DNA primase in coupling DNA replication to DNA damage response. *EMBO J.*, **16**, 639–650.
82. Branzei,D. and Foiani,M. (2005) The DNA damage response during DNA replication. *Curr. Opin. Cell Biol.*, **17**, 568–575.
83. Lemacon,D., Jackson,J., Quinet,A., Brickner,J.R., Li,S., Yazinski,S., You,Z., Ira,G., Zou,L., Mosammaparast,N. *et al.* (2017) MRE11 and EXO1 nucleases degrade reversed forks and elicit MUS81-dependent fork rescue in BRCA2-deficient cells. *Nat. Commun.*, **8**, 860–872.
84. Pike,J.E., Burgers,P.M., Campbell,J.L. and Bambara,R.A. (2009) Pif1 helicase lengthens some Okazaki fragment flaps necessitating Dna2 nuclease/helicase action in the two-nuclease processing pathway. *J. Biol. Chem.*, **284**, 25170–25180.
85. Budd,M.E., Reis,C.C., Smith,S., Myung,K. and Campbell,J.L. (2006) Evidence suggesting that Pif1 helicase functions in DNA replication with the Dna2 helicase/nuclease and DNA polymerase delta. *Mol. Cell. Biol.*, **26**, 2490–2500.
86. Burgers,P.M. (2009) Polymerase dynamics at the eukaryotic DNA replication fork. *J. Biol. Chem.*, **284**, 4041–4045.
87. Rossi,S.E., Foiani,M. and Giannattasio,M. (2018) Dna2 processes behind the fork long ssDNA flaps generated by Pif1 and replication-dependent strand displacement. *Nat. Commun.*, **9**, 4830–4841.
88. Andersen,S.D., Keijzers,G., Rampakakis,E., Engels,K., Luhn,P., El-Shemerly,M., Nielsen,F.C., Du,Y., May,A., Bohr,V.A. *et al.* (2012) 14-3-3 checkpoint regulatory proteins interact specifically with DNA repair protein human exonuclease 1 (hEXO1) via a semi-conserved motif. *DNA Repair (Amst.)*, **11**, 267–277.
89. Chen,X., Kim,I.K., Honaker,Y., Paudyal,S.C., Koh,W.K., Sparks,M., Li,S., Piwnica-Worms,H., Ellenberger,T. and You,Z. (2015) 14-3-3 proteins restrain the Exo1 nuclease to prevent overresection. *J. Biol. Chem.*, **290**, 12300–12312.
90. Orans,J., McSweeney,E.A., Iyer,R.R., Hast,M.A., Hellinga,H.W., Modrich,P. and Beese,L.S. (2011) Structures of human exonuclease 1 DNA complexes suggest a unified mechanism for nuclease family. *Cell*, **145**, 212–223.
91. Chen,X., Paudyal,S.C., Chin,R.I. and You,Z. (2013) PCNA promotes processive DNA end resection by Exo1. *Nucleic Acids Res.*, **41**, 9325–9338.
92. Zhang,F., Shi,J., Chen,S.H., Bian,C. and Yu,X. (2015) The PIN domain of EXO1 recognizes poly(ADP-ribose) in DNA damage response. *Nucleic Acids Res.*, **43**, 10782–10794.
93. Gardino,A.K., Smerdon,S.J. and Yaffe,M.B. (2006) Structural determinants of 14-3-3 binding specificities and regulation of subcellular localization of 14-3-3-ligand complexes: a comparison of the X-ray crystal structures of all human 14-3-3 isoforms. *Semin. Cancer Biol.*, **16**, 173–182.
94. Chappidi,N., De Gregorio,G. and Ferrari,S. (2019) Replication stress-induced Exo1 phosphorylation is mediated by Rad53/Pph3 and Exo1 nuclear localization is controlled by 14-3-3 proteins. *Cell Div.*, **14**, 1.
95. Keijzers,G., Liu,D. and Rasmussen,L.J. (2016) Exonuclease 1 and its versatile roles in DNA repair. *Crit. Rev. Biochem. Mol. Biol.*, **51**, 440–451.
96. Axelsen,J.B., Lotem,J., Sachs,L. and Domany,E. (2007) Genes overexpressed in different human solid cancers exhibit different tissue-specific expression profiles. *Proc. Natl. Acad. Sci. U.S.A.*, **104**, 13122–13127.
97. Dai,Y., Tang,Z., Yang,Z., Zhang,L., Deng,Q., Zhang,X., Yu,Y., Liu,X. and Zhu,J. (2018) EXO1 overexpression is associated with poor prognosis of hepatocellular carcinoma patients. *Cell Cycle*, **17**, 2386–2397.